Meteorological responses of carbon dioxide and methane fluxes in the terrestrial and aquatic ecosystems of a subarctic landscape

Lauri Heiskanen[1], Juha-Pekka Tuovinen[1], Henriikka Vekuri[1], Aleksi Räsänen[2,3], Tarmo Virtanen[2], Sari Juutinen[2,4], ~~Henriikka Vekuri[1],~~ Annalea Lohila[1], Juha Mikola[2,~~5~~3], Mika Aurela[1]

5   [1]Climate System Research Unit, Finnish Meteorological Institute, Helsinki, Finland
[2]Ecosystems and Environment Research Programme, Faculty of Biological and Environmental Sciences, University of Helsinki, Helsinki, Finland
[3]Natural Resources Institute Finland (LUKE), Oulu, Finland
[4]University of Eastern Finland, Department of Geographical and Historical Studies, Joensuu, Finland
10   [5]Natural Resources Institute Finland (LUKE), Helsinki, Finland

Correspondence to: Lauri Heiskanen (lauri.heiskanen@fmi.fi)

Abstract

The subarctic landscape consists of a mosaic of forest, peatland and aquatic ecosystems and their ecotones. The carbon (C)
15   exchange between ecosystems and the atmosphere through carbon dioxide (CO_2) and methane (CH_4) fluxes varies spatially and temporally among these ecosystems. Our study area in Kaamanen in northern Finland covered 7 km^2 of boreal subarctic landscape with upland forest, open peatland, pine bogs and lakes. We measured the CO_2 and CH_4 fluxes with eddy covariance and chambers between June 2017 and June 2019 and studied the C flux responses to varying meteorological conditions. The landscape area was an annual CO_2 sink of -45 ± 22 and -33 ± 23 g C m^{-2} and a CH_4 source of 3.0 ± 0.2 and 2.7 ± 0.2 g C m^{-2}
20   during the first and second study year, respectively. The pine forest had the largest contribution to the landscape-level CO_2 sink, -126 ± 21 and -101 ± 19 g C m^{-2}, and the fen to the CH_4 emissions, 7.8 ± 0.2 and 6.3 ± 0.3 g C m^{-2}, during the first and second study year, respectively. ~~The landscape area was an annual CO_2 sink of -25.9 ± 65.7 and -41.3 ± 64.9 g C m^{-2}, and a CH_4 source of 2.4 ± 0.7 and 2.3 ± 0.7 g C m^{-2} during the first and second study year, respectively. The pine forest had the largest contribution to the landscape-level CO_2 sink, -78.3 ± 50.8 and -118.9 ± 26.8 g C m^{-2}, and the fen to the CH_4 emissions,~~
25   ~~7.0 ± 0.2 and 6.3 ± 0.3 g C m^{-2}, during the first and second study year, respectively.~~ The lakes within the area acted as CO_2 and CH_4 sources to the atmosphere throughout the measurement period, and a lake located downstream from the fen having organic sediment showed fourfold fluxes compared to a mineral sediment lake. ~~The lakes within the area acted as CO_2 and CH_4 sources to the atmosphere throughout the measurement period, with an organic sediment lake located downstream from the fen showing sixfold fluxes compared to a mineral sediment lake.~~ The annual C balances were affected most by the rainy
30   peak growing season in 2017, the warm summer in 2018 and a heatwave and drought event in July 2018. The rainy period increased ecosystem respiration (ER) in the pine forest due to continuously high soil moisture content, and ER was on a level similar to the following, notably warmer summer. A corresponding ER response to abundant precipitation was not observed

for the fen ecosystem, which is adapted to high water table levels, and thus a higher ER sum was observed during the warm summer 2018. ~~The annual C balances were affected most by the rainy peak growing season of 2017 and the heatwave and drought event in July 2018. The rainy period increased the ecosystem respiration of the pine forest due to continuously high soil moisture content. A similar flux response to abundant precipitation was not observed for the fen ecosystem, which is adapted to high water table levels.~~ During the heatwave and drought period, similar responses were observed for all terrestrial ecosystems, with decreased gross primary productivity and net CO_2 uptake, caused by the unfavourable growing conditions and plant stress due to the soil moisture and vapour pressure deficits. Additionally, the CH_4 emissions from the fen decreased during and after the drought. However, the timing and duration of drought effects varied between the fen and forest ecosystems, as C fluxes were affected sooner and had a shorter post-drought recovery time in the fen than forest~~s~~. The differing CO_2 flux response to weather variations showed that terrestrial ecosystems can have a contrasting impact on the landscape-level C balance in a changing climate, even if they function similarly most of the time.

1 Introduction

A typical boreal subarctic landscape consists of a mosaic of land cover types including forests, open and forested peatlands and water bodies, with each ecosystem acting as a source or sink of atmospheric carbon (C) depending on its characteristics and weather conditions. To grasp a full picture of the C balance at the landscape scale, the carbon dioxide (CO_2) and methane (CH_4) exchange between the main ecosystems and the atmosphere needs to be assessed. This is also because part of the C fixed in terrestrial systems can be emitted back to the atmosphere via aquatic ecosystems or transported out from the catchment. The net atmosphere-ecosystem CO_2 exchange is a result of gross primary production (GPP) of plants and ecosystem respiration (ER), which is composed of autotrophic and heterotrophic respiration (Chapin et al., 2011). The CH_4 emissions from ecosystems are mainly produced by methanogens in the waterlogged, ~~anaerobic~~ anoxic zone in soils, while the CH_4 uptake is caused by oxidation by methanotrophs in aerobic soil conditions (Le Mer and Roger, 2001).

As a result of the ongoing climate change, the subarctic regions warm rapidly, two to three times as fast as the rest of the world (Masson-Delmotte et al., 2018). The higher temperatures affect the C cycle of subarctic ecosystems by lengthening the growing season and shortening the snow and ice cover periods. Higher temperatures and a longer growing season enable greater CO_2 uptake through photosynthesis (Aurela et al., 2004; Silvfer et al., 2020), but they also allow greater CO_2 emissions due to the increased heterotrophic and autotrophic respiration (Kätterer et al., 1998). However, the variation in ecosystem C dynamics is also highly dependent on water balance, as too low a moisture content in soils decreases GPP and decomposition of organic matter (Jones, 2013; Meyer et al., 2018), and methanogenesis requires anoxic soil conditions (Chapin et al., 2011). In aquatic ecosystems, the longer ice-free periods, with increased C input from surrounding terrestrial ecosystems, lead to higher annual C emissions to the atmosphere (Cole et al., 2007, Guo et al., 2020). In a longer than one-year timespan, the effects of climate change are observed as vegetation composition shifts, such as Arctic shrubification that enhances CO_2 uptake and alters

ecosystem respiration and nutrient availability (Mekonnen et al., 2021). Concurrently, the potential of severe weather events,

65 such as heatwaves and droughts, to affect the C cycles increases within the region (Masson-Delmotte et al., 2018).

Boreal upland forests have been shown to act as either annual net sinks or sources of atmospheric CO_2, depending on species composition, climatic conditions and the occurrence of extreme weather events, fires, and herbivories and pathogens (Bond-Lamberty et al., 2007; Kljun et al., 2007; Lindroth et al., 2008; Aurela et al., 2015; Hadden and Grelle, 2017), and these ecosystems usually act as small CH_4 sinks (Dinsmore et al., 2017). Undrained boreal peatlands have been, in a long term, net

70 CO_2 sinks via accumulation of organic C, but similarly to forests their annual CO_2 balance is sensitive to environmental conditions (Bubier et al., 1998; Aurela et al., 2004; Lindroth et al., 2007). Additionally, these peatlands release CH_4 into the atmosphere (Chapin et al., 2011). Peatlands have more C stored in the soil, but less C in living plant matter compared to upland forests, and thus the same disturbances on the ecosystems can lead to differing effects on the C balance.

Globally, inland waters act as net CO_2 and CH_4 sources to the atmosphere (Tranvik et al., 2009). Boreal lakes vary greatly in

75 their area and depth, input of organic and inorganic C from the terrestrial ecosystems, ice-free period duration and the amount of C in sediments and aquatic vegetation, which all affect the magnitude of the C exchange with the atmosphere (Bastviken et al., 2004; Wik et al., 2018; Denfeld et al., 2020). Additionally, water bodies provide paths for lateral flow of water, C and other matter between ecosystems (Cole et al., 2007).

The landscape-level C balance comprised of diverse ecosystems is evidently dependent on the ecosystem composition, and the

80 regional effect of an environmental change or disturbance depends on the integrated response of individual ecosystems. As an example of such a disturbance, a heatwave and drought event encompassed north-western Europe during the summer of 2018 (Lehtonen and Pirinen, 2019 a, b). The drought conditions had different effects on the CO_2 exchange of boreal forests and peatlands in the area (Rinne et al., 2020; Lindroth et al., 2020; Matkala et al., 2021). There was large variation in how different forests reacted to the heatwave and drought, some showing a substantial decrease and some no change or even an increase in

85 CO_2 uptake (Lindroth et al., 2020; Matkala et al., 2021). Most of the studied peatlands turned momentarily into CO_2 sources during the drought, which lowered their annual CO_2 uptake significantly, and simultaneously the CH_4 emissions decreased (Rinne et al., 2020). Thus, the landscape-level C balance depends on multiple responses, whose net effects are not easily predictable.

In this study, we assess the ecosystem-atmosphere exchange of CO_2 and CH_4 within a subarctic landscape based on eddy

90 covariance and chamber measurements. The studied area in Kaamanen in northern Finland includes an upland pine forest, pine bogs, a mesotrophic flark fen and shallow lakes of glacial origin. We focus on the temporal variation of C exchange during two full years (June 2017 – June 2019). The meteorological conditions during the first year were similar to the long-term average, with the exception of the higher-than-average precipitation sum in summer. The second year included the above-mentioned heatwave and drought period. Motivated by the plant community-level study of Heiskanen et al. (2021), who found

95 that the diversity of plant communities constrained C loss from the Kaamanen fen during the 2018 drought, we study if a similar pattern can be observed at the ecosystem level.

Here, we address questions on how sensitive the C fluxes of different ecosystems are to changes in environmental conditions and how this is reflected on the landscape-level C exchange. The more specific scientific questions addressed are: (1) What are the contributions of each ecosystem to the landscape-level CO_2 and CH_4 fluxes? (2) Do the CO_2 and CH_4 fluxes of different ecosystems show similar responses to varying meteorological conditions?

2 Materials and methods

2.1 Study site

The studied landscape is located in Kaamanen in northern Finland (69°8' N, 27°16' E; 155 m a.s.l.) within the subarctic climate zone and the northern boreal vegetation zone. The annual mean temperature in the region was -0.4 °C and the mean annual precipitation sum 472 mm in 1981–2010 (Pirinen et al., 2012). Even though the study area is located within the sporadic permafrost zone, no permafrost has been found there anymore in recent decades (Fronzek et al., 2010). The growing season is short and lasts for 150–180 days (Aurela et al., 2002). The study area covers 7 km^2 around the flux measurement sites (Fig. 1) and consists of five main ecosystem types: upland pine forest, patterned mesotrophic flark fen, treed pine bog, sparsely treed pine bog, and lakes and a connecting stream (Fig. 2). The ecosystems within the study area are homogeneous in their species composition and provide a representative sample of the landscape.

The areal coverage of different ecosystem types in the landscape was estimated with a land cover classification utilizing remote sensing data and field observations following the methodology described by Räsänen and Virtanen (2019). An aerial orthophoto was segmented, 55 features for each segment were calculated from multi-source remote sensing data, including orthophoto, aerial laser scanning and satellite imagery, and a supervised random forest classification (Breiman 2001) was carried out using field data for model training and validation (Sect. S.1 in the Supplement S.1). The pine forest, pine bog, fen and lake ecosystems each encompass roughly an equal area (Table 1). The ecosystems in the area are pristine with the exception of some forest loggings, thinning and selective removal of birches in part of the pine-dominated forests.

The mesotrophic patterned flark fen is an open peatland ecosystem characterised by a mosaic of string and flark microforms,. with tThe 0.5–1 m high string formations are 0.5–1 m high and can remain frozen until the late summer (Aurela et al., 2001). The fen vegetation has also a clear patterning and can be partitioned to five distinct plant community types (PCTs) that differ in their vegetation composition, water table level and carbon fluxes: flark, *Trichophorum* tussock, string margin, string top and tall sedge fen (Maanavilja et al., 2011; Räsänen et al. 2019; Heiskanen et al., 2021). In the flarks, the plant communities are dominated by sedges, including *Trichophorum* tussocks, and brown mosses. The top of the strings act as ombrotrophic bog-like surfaces within the fen and are covered mainly by dwarf shrubs, herbs, mosses and lichens, while string margins are populated by dwarf birch (*Betula nana)* and other dwarf shrubs, sedges and *Sphagnum* mosses. The fifth PCT, a tall sedge fen that is covered by tall sedges, deciduous shrubs and forbs, can be found in the riparian areas of lakes and small streams. The species composition of these PCTs was described in detail by Maanavilja et al. (2011) and Räsänen et al. (2019), and paleorecords by Piilo et al. (2020). The bedrock under the peatland slopes towards the south. The average peat thickness

4

increases from 1 m in the northern part of the fen towards the south, where it is up to 4 m (Piilo et al., 2020). Most of the aboveground biomass of the peatland resides in shrubs and mosses, and forbs and graminoids contribute increasingly to the total leaf area in the mid and late growing season (Table A1).

The dominant tree species in the upland mineral soil forest is Scots pine (*Pinus sylvestris*) with a few downy birch (*Betula pubescens*) trees also present (Table A2). The forest around the flux measurement site was logged about 50 yr ago, but most of the pine forests within the study area are pine-dominated old-growth forest with an uneven age distribution. The average heights of all trees and the main canopy were approximately 8 and 11 m, respectively (Table A32). The field layer is dominated by evergreen dwarf shrubs (e.g. *Vaccinium vitis-idaea* and *Calluna vulgaris*), and the ground layer is covered by mosses and lichens. The soil type in the forest is sandy podzol, which has higher bulk density, lower nitrogen (N) content and higher C:N ratio than the soil in the peatlands (Table A43, Sect S.2 in the Supplement). Mosses and lichens contribute about 10 % to the total aboveground biomass (Table A1, A5).

The tree height and density decrease from the upland pine forest to the pine bog ecosystems. The average tree height in the pine bog was 5 m, and in treed pine bog and sparsely treed pine bog the above-ground tree biomass was about 50 % and 16 %, respectively, of the biomass in pine forest (Tables A32, A54). The field layer vegetation of the pine bog ecosystems is similar to that of the string tops (Table A1), with evergreen (*Ledum palustre*) and deciduous (*Vaccinium uliginosum* and *Betula nana*) shrubs, herbs (*Rubus chamaemorus*) and graminoids (mostly *Carex* spp.). The pine bog ground layer is formed by mosses and a few lichens. The soil carbon content is higher in the sparsely treed bog patches within the fen than in bog vegetation with thinner organic layer at the forest edge. Soil N content and C:N ratio are similar to those found in pine forest and string tops (Table A43).

The water bodies within the study area vary in size from small streams and ponds to lakes larger than 25 ha (Lake Ulkujärvi in the northwest and Lake Jänkäjärvi in the south, Fig. 1). The lakes in the area are shallow, the depth ranging from less than 1 m to a few metres and have a sandy or organic sediment bottom. Most water bodies in the study area belong to the same catchment, with water flowing from north to south. The aquatic vegetation is sparse, near the shore consisting of macrophytes, mainly horsetail (*Equisetum fluviatile*), sedges (*Carex* spp.), *Menyanthes trifoliata* and benthic algae. A few-metre-wide stream flows through the peatland and connects Lake Ulkujärvi to Lake Jänkäjärvi. Additionally, water flows on the surface across the fen and through the peat layers and eskers. Each year, during the spring thaw, the fen and partially the pine bogs become flooded.
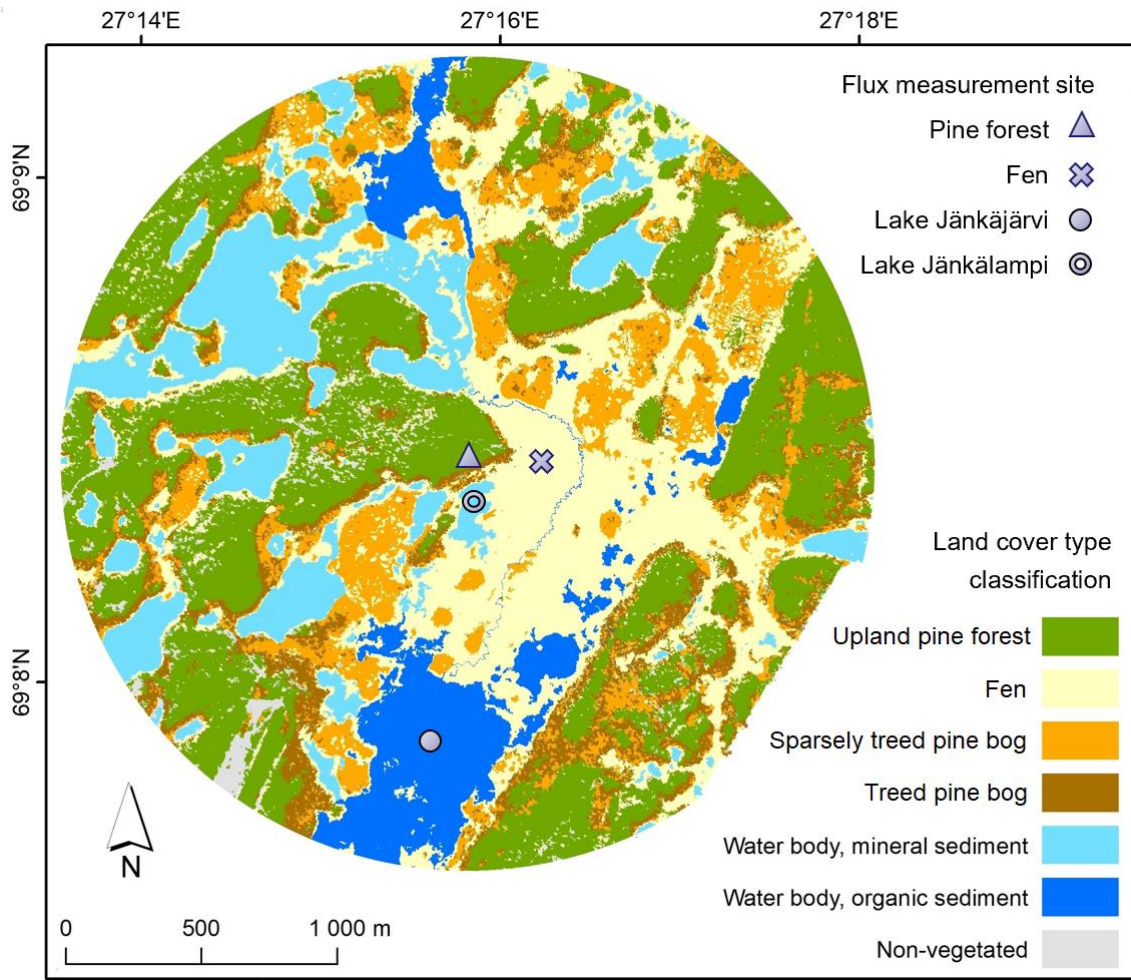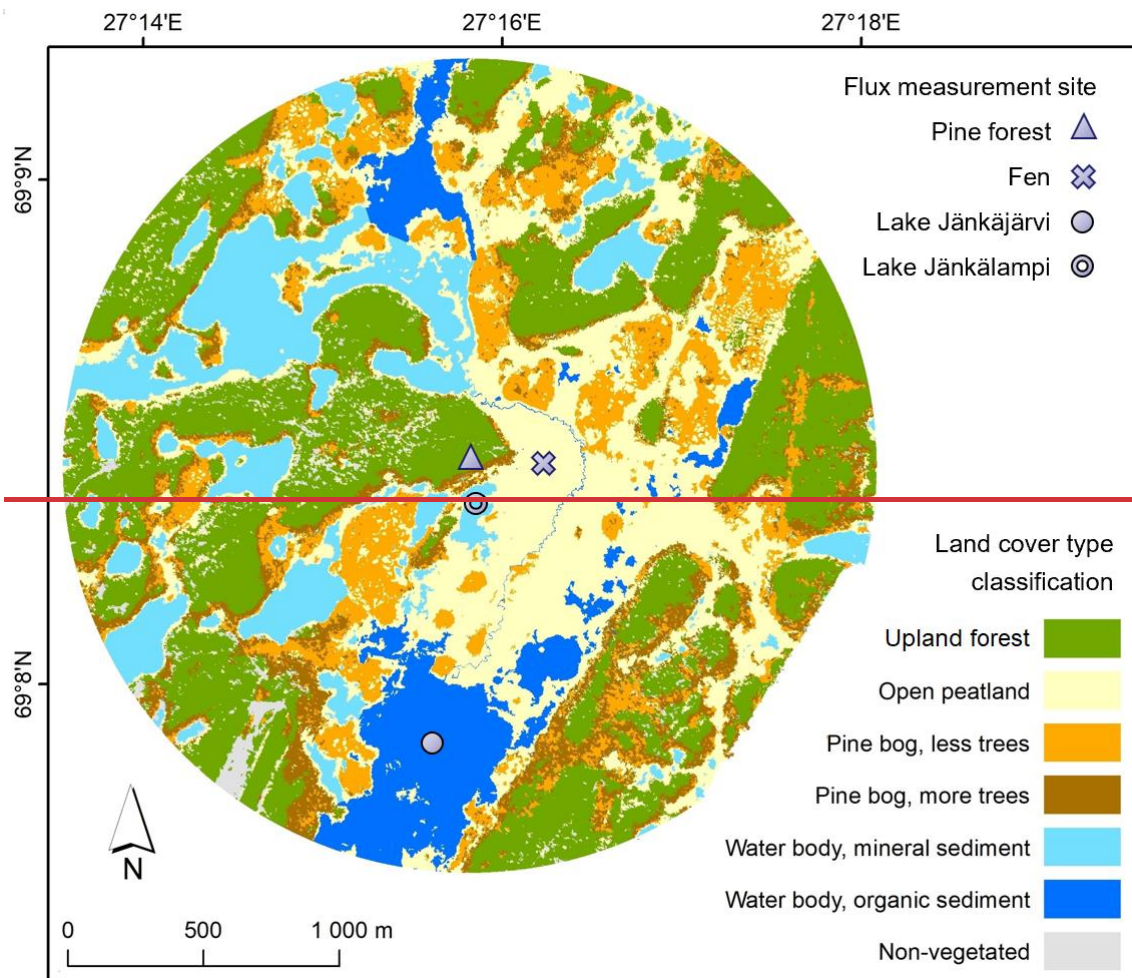
Figure 1. The study area in Kaamanen with land cover type classification and flux measurement site locations.

Table 1. Relative areal coverage of the land cover types within the study area.

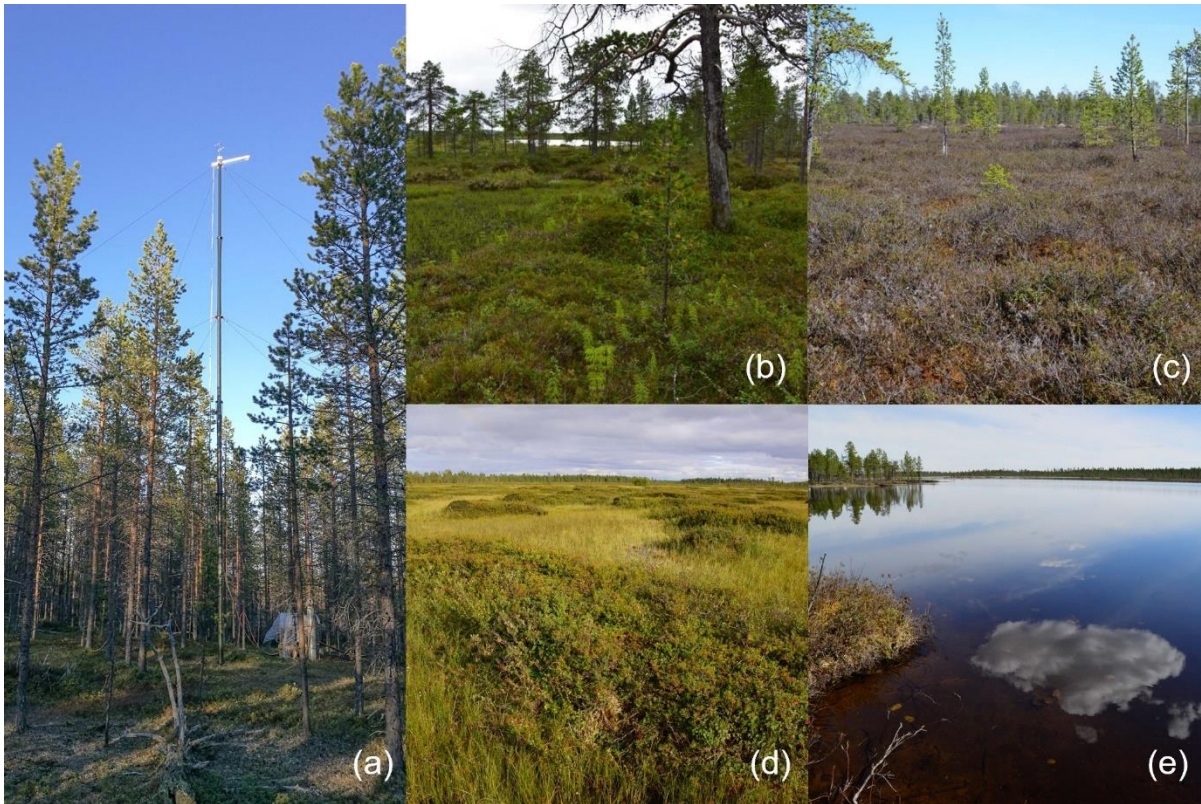| Land cover type	Areal coverage [%]
Upland pine forest	29.2
Treed pine bogPine bog, more trees	9.1
Sparsely treed pine bogPine bog, less trees	13.5
FenOpen peatland	26.1
Water body, mineral sediment	12.5
Water body, organic sediment	7.8

Non-vegetated	1.8

Figure 2. The main ecosystem types within the study area: (a) Scots pine forest, (b) treed pine bog, (c) sparsely treed pine bog, (d) fen and (e) lake ecosystems. Photo: (a) Lauri Heiskanen, (b)-(e) Tarmo Virtanen.

2.2 Flux measurement methods

2.2.1 Pine forest CO$_2$ flux measurements

The CO$_2$ flux measurements in the Scots pine forest were set up in the beginning of the growing season in 2017, and data acquisition was started on 8 June 2017. The eddy covariance (EC) measurements were conducted on a 14 m tall tower that was located on the southern edge of the forest so that in the wind sector 250°–65° the forest coverage was higher than 80 %. The EC system consisted of a three-axis sonic anemometer (USA-1, METEK Meteorologische Messtechnik GmbH, Germany) and a closed-path infrared gas analyser for CO$_2$ and H$_2$O mixing ratios (LI-7200, LI-COR Biosciences, USA). The inlet tube for the gas analyser was ~18 m long and had an inner tube diameter of 3.1 mm. The flow rate was 5–6 L min^{-1}.

The sampling frequency for the EC flux data was 10 Hz. Standard methods were used for calculating the half-hourly turbulent fluxes (Aubinet et al., 2012), with block averaging and a double rotation of the coordinate system (McMillen, 1988). The high-

frequency signal attenuation flux losses were taken into account using an experimental transfer function with a half-power frequency of 1.9 Hz (Laurila et al., 2005).

The half-hourly averaged data were accepted based on the following screening criteria: relative stationarity $< 100\%$ (Foken and Wichura, 1996), number of recorded data per 30 min $> 17\,400$, number of signal spikes per 30 min < 360, mean CO_2 mixing ratio within 340–550 ppm. A friction velocity (u_*) limit of 0.24 m s^{-1} was used for screening the periods of insufficient turbulence. Data from the wind direction sector 250°–65° were used to calculate the CO_2 balances of the forest.

As the net ecosystem exchange of CO_2 in forests (NEE_{forest}) can be significantly affected by the flux due to storage change below the measurement height, this was estimated according to Montagnani et al. (2018) and added to the measured eddy flux (F_{CO_2}):

$$NEE_{forest} = F_{CO_2} + \overline{\rho_d} \frac{\overline{\Delta CO_2}}{\Delta t} h \tag{1}$$

where $\overline{\rho_d}$ is the mean dry air density, $\frac{\overline{\Delta CO_2}}{\Delta t}$ is the change of CO_2 dry molar fraction at the EC measurement height during the 30 min averaging period, and h is the measurement height. The CO_2 concentration profile below the measurement height was assumed to be constant.

2.2.2 Fen CO_2 and CH_4 flux measurements

The CO_2 and CH_4 fluxes of the Kaamanen fen were measured with both the EC and flux chamber methods. The EC measurements were used for the fen ecosystem flux analysis here, and the PCT-specific chamber-based data were used for estimating the CO_2 fluxes of the pine bog ecosystems. Even though the fen is comprised of a mosaic of different PCTs, the contribution of each type is similar in all wind directions within a 100–150 m radius, and thus the footprint variation is not expected to bias the ecosystem balances derived from EC measurements.

The measurements were conducted on a 5 m tall tower with a three-axis sonic anemometer (USA-1, METEK Meteorologische Messtechnik GmbH, Germany), a closed path infrared gas analyser for CO_2 and H_2O mixing ratios (LI-7000, LI-COR Biosciences, USA) and a laser-based gas analyser for CH_4 mixing ratio (RMT-200, Los Gatos Research, USA). The heated inlet tubes (inner diameter 3.1 mm and 8 mm for LI-7000 and RMT-200, respectively) were 6 m long and had a flow rate of 6 L min^{-1} and 15 L min^{-1} for the LI-7000 and RMT-200, respectively. The sampling frequency was 10 Hz for both analysers. The same flux calculation and data processing methods were used as with the pine forest EC data, except for the discarded wind direction sector (260°–315°), the u_* limit (0.1 m s^{-1}) and the relative stationarity limit (30 %) (Foken and Wichura, 1996); in addition, a mean CH_4 mixing ratio of 1.8–2.8 ppm was required.

The manual chamber measurements were conducted bi-weekly in 12 June – 11 October 2017 and 31 May – 4 September 2018 on four main plant communities that grow on the microtopography gradient (flark, *Trichophorum* tussock, string margin and string top). A total of 17 chamber plots were used with four or five replicates on each PCT. For determining the ER flux and the light response of CO_2 flux, a transparent chamber was used with one to three shading elements over the chamber. The chamber was closed for 2 min during each measurement, and the CO_2 and CH_4 fluxes were calculated from the mixing ratio

change measured inside the chamber. The EC and chamber measurements at the fen and the PCT-specific fluxes are presented in more detail by Heiskanen et al. (2021).

~~The measurements were conducted on a 5 m tall tower with a three-axis sonic anemometer (USA-1, METEK Meteorologische Messtechnik GmbH, Germany), a closed-path infrared gas analyser for CO_2 and H_2O mixing ratios (LI-7000, LI-COR Biosciences, USA) and a laser-based gas analyser for CH_4 mixing ratio (RMT-200, Los Gatos Research, USA). The same flux calculation and data processing methods were used as with the pine forest EC data, except for the discarded wind direction sector (260°–315°) and the friction velocity limit (0.1 m s^{-1}).~~

~~The manual chamber measurements of the main plant communities were conducted during the growing season in 2017 and 2018.~~

For modelling the string top CO_2 fluxes for the time span from June 2017 to June 2019, to be used for pine bog (Sect. 2.4), the chamber-based fen ecosystem fluxes were scaled to match the EC-based fen fluxes. This was done similarly to Piilo et al. (2020) by first upscaling the chamber fluxes of the main PCTs of the fen to the ecosystem scale according to their relative areas within 200 m from the EC tower (Table 2). The PCT-specific fluxes were presented in more detail by Heiskanen et al. (2021).

The mean ratio~~s~~ between the EC-based and ~~fen ecosystem scale~~upscaled chamber-based ER and GPP fluxes ~~and the fen EC fluxes~~ were used for scaling the chamber flux~~es calculated from the~~ data ~~measured during the manual chamber measurement days~~ (Table 3). ~~The~~For ER, the mean ratio was calculated ~~by~~from all ~~using the 24 h~~ data, while the mean GPP ratio was calculated ~~by using only~~from the daytime data (from 6 a.m. to 6 p.m. local standard time).

Table 2. Area coverage of the plant community types of the peatland inside a 200 m radius around the eddy covariance tower.

Plant community type	Area coverage [%]
Flark	37
Trichophorum tussock	10
Tall sedge fen	17
String margin	14
String top	16
Pine bog	6

~~The mean ratio between the fen ecosystem scale chamber-based ER and GPP fluxes and the fen EC fluxes were used for scaling the chamber fluxes calculated from the data measured during the manual chamber measurement days (Table 3). The ER ratio was calculated by using the 24 h data, while the GPP ratio was calculated by using only the daytime data from 6 a.m. to 6 p.m. local standard time.~~

Table 3. ~~The scaling c~~Coefficients ~~used~~ for scaling the chamber-based ER and GPP ~~chamber~~ fluxes.

Time period	ER ratio	GPP ratio
June 2017 – October 2017	1.170~~1.367~~	1.514~~1.620~~
November 2017 – April 2018	1.012~~1.142~~	1.337~~1.387~~
May 2018 – June 2019	0.854~~0.918~~	1.160~~1.154~~

2.2.3 Eddy covariance data gap-filling and partitioning

The EC flux time series of both the pine forest and fen ecosystems had substantial gaps due to equipment failures, wind sector exclusions and quality control filtering applied during the post-processing of data. ~~The gaps in the CO_2 flux data were filled by GPP and ER flux values modelled with environmental response functions, as described by Heiskanen et al. (2021). A rectangular hyperbola was used to model the dependency of GPP on photosynthetic photon flux density (PPFD), while the exponential Lloyd-Taylor (1994) model was used for ER. For the pine forest flux parameterisation, air temperature was used during the growing season, while soil temperature (T_s) at the 10 cm depth was used for the other periods, while for the fen, T_s at the 10 cm depth was used for the whole year.~~

~~The fitting of the GPP function was performed in a moving window with a minimum of 3 days and 30 half-hourly observations of the daytime flux data (PPFD > 30 μmol m^{-2} s^{-1}). For fitting the parameters of the ER function, night-time data were used (PPFD < 30 μmol m^{-2} s^{-1}). The respiration activation energy parameter (E_0) was fitted first with a 91-day moving window, after which the base respiration rate at 10 °C (R_{10}) was fitted to the data within a moving window of at least 7 days.~~

~~A long gap in the pine forest EC flux data in April-June 2019 was filled by utilizing the response function parameters estimated for the same period in 2018.~~ In total, 86 % and 91 % of the forest CO_2 flux data were gap filled in the time series of 11 June 2017 – 10 June 2018 and 11 June 2018 – 10 June 2019, respectively. During the growing seasons, i.e. in 11 June – 31 October 2017 and 11 June – 31 October 2018, the gap-filling percentage was 77 % and 84 %, respectively. In total, 64 % and 63 % of the fen CO_2 flux data were gap-filled in the time series of the first and second year, respectively. ~~The wind direction screening created 43 percentage points of the missing data.~~ The contribution of each data filtering step is shown in Table S1 in the Supplement.

For gap-filling the pine forest CO_2 fluxes during the winter, when the data coverage was lowest but the fluxes relatively small and stable, we averaged the measurement data pooled into two soil temperature categories, over and under -2 °C at the 10 cm depth. The mean fluxes were 0.0173 and 0.0103 mg CO_2 m^{-2} s^{-1} in the warmer and colder category, respectively. The winter period was determined based on the timing of frost at 10 cm depth, which occurred in 31 September 2017 – 24 April 2018 and 30 September 2018 – 20 April 2019.

The growing season pine forest CO_2 flux data and the entire fen CO_2 flux data time series were gap-filled using a machine learning method called extreme gradient boosting (XGBoost, Chen and Guestrin, 2016). XGBoost is a decision tree-based ensemble method in which trees are built in a sequential manner so that each tree corrects for the errors of the previous trees. XGBoost has been shown to perform well even with long gaps in the EC data (Zhu et al., 2022; Irvin et al., 2021). The

11

environmental variables that were used to predict NEE were photosynthetic photon flux density (PPFD), air temperature, relative humidity, vapour pressure deficit (VPD), soil temperature at -10 cm, soil temperature at -5 cm and soil moisture at -10 cm.

First, we optimized the hyperparameters of the model using grid search to control for overfitting and to select the best model architecture. The hyperparameters that were optimized control for the maximum depth of a tree ('max_depth'), the subsample ratio of columns when constructing each tree ('colsample_bytree'), learning rate ('learning_rate') and the minimum number of samples required to create a new node in a tree ('min_child_weight'). The selected hyperparameters were 0.8 for 'colsample_bytree', 0.05 for 'learning_rate', 20 for 'max_depth' and 9 for 'min_child_weight'. The squared error was used as the loss function. Model performance for the more sparse pine forest data was evaluated using 10-fold cross validation, resulting in the coefficient of determination (R^2) of 0.88 ± 0.02 and the mean squared error of 0.003 ± 0.0006 mg CO_2 m^{-2} s^{-1} (Fig. S3 in the Supplement). Further details of model performance and justification for gap-filling the EC flux time series with a high proportion of missing data are presented in Sect. S.3 in the Supplement.

The ER and GPP fluxes were partitioned based on environmental response functions that were fitted to the gap-filled NEE data. A rectangular hyperbola was used to model the dependency of GPP on PPFD (e.g. Whiting, 1994), while the exponential model of Lloyd and Taylor (1994) was used for ER. For the pine forest flux parameterisation, air temperature was used during the growing season, while soil temperature (T_s) at the 10 cm depth was used for the other periods; for the fen, T_s at the 10 cm depth was used for the whole year. For fitting the parameters of the ER function, night-time data were used (PPFD < 30 µmol m^{-2} s^{-1}). The activation energy parameter (E_0) of the respiration function was fitted first with a 91-day moving window, after which the base respiration rate at 10 ºC (R_{10}) was fitted to the data within a moving window of 7 days. The fitting of the GPP function was performed in a moving window of 3 days using the daytime flux data (PPFD > 30 µmol m^{-2} s^{-1}).

The EC CO_2 fluxes of the fen were gap-filled similarly to the pine forest fluxes. In total, 64 % and 63 % of the fen CO_2 flux data were gap-filled in the time series of the first and second year, respectively. For gap-filling the CH$_4$ fluxes measured at the fen, a simple moving average interpolation of the half-hour fluxes was used. A moving average window of $\pm$ 1, 2, 4, 8, 16 or 32 d was used depending on the length of the gaps in data. In total, 69 % and 70 % of the CH$_4$ flux data were gap-filled in the time series of the first and second year, respectively (Table S1 in the Supplement).

2.2.4 Lake CO_2 and CH$_4$ flux measurements

The diffusive fluxes of CO_2 and CH$_4$ were measured on the intermediate-sized (1.5 ha) Lake Jänkälampi with mineral sediment and on the larger Lake Jänkäjärvi with organic sediment (Fig. 1). On Jänkäjärvi, also CH$_4$ ebullition was measured. The lakes are hereafter referred to as the MS and OS lakes, respectively. The diffusive fluxes of CO_2 and CH$_4$ were measured on the intermediate side (1.5 ha) mineral sediment Lake Jänkälampi (Fig. 1), hereafter referred to as the MS lake, during the ice-free periods in 2017 and 2018. The diffusive fluxes of these glasses and the CH$_4$ ebullition flux were measured at the larger, organic sediment Lake Jänkäjärvi (Fig. 1), hereafter referred to as the OS lake, during summer 2017. The MS lake fluxes were measured on five days between during June and October in 2017 and other five days between during June and September

12

2018. The OS lake ~~fluxes were~~was measured biweekly during June – August 2017. ~~The second year of the organic sediment~~

~~(OS) lake were estimated by using the first year's measurements. The estimated second year OS lake fluxes were used for~~

~~assessing the landscape level fluxes.~~

The flux measurements were conducted with floating flux chambers, while the CH_4 ebullition was determined from both chamber and floating bubble collector data. The diffusive fluxes of the MS lake were measured with an opaque aluminium chamber (60 cm × 60 cm × 30 cm) at 20 m from the north shore. The chamber air was mixed with a battery-driven fan. The closure time was 7 min, after which the chamber was ventilated for 3 min. The changes in CO_2, CH_4 and H_2O mixing ratios inside the chamber were measured using a closed-path ~~infrared~~ laser-based gas analyser (Picarro G2401, Picarro Inc, USA) connected to the chamber via a 50 m long inlet tube (Teflon, inside diameter 3.1 mm). On the OS lake, floating chambers with a volume of 8 L and an area of 0.05 m^2 were applied, using a 30~~–~~60 min closure. Four samples (30 mL) of gas space were drawn using polyethene syringes, and the samples were stored in 12 mL glass vials flushed with sample air. Samples were analysed within a month using a gas chromatograph equipped with electron capture, thermal conductivity and flame ionization detectors ~~EC, TC and FI detectors~~ (Agilent 7890B, with Gilson GX271 autosampler). We tested CO_2 ~~concentrations and~~ fluxes against those ~~measured~~ determined using an on-line CO_2 sensor (K33 ELG CO_2 module, Senseair) in ~~one~~ three of the chambers, and obtained similar flux values. In all, five to ten chambers were deployed at ~~the~~ a time. The chambers were lined with a rope, anchored in both ends, so that they captured open water section of the lake from ~~a water segment extending from about 20 m~~ ~~from~~ near shore towards the lake centre. The chambers captured some ebullition events, and these were ~~accounted~~ included as bubble flux. In addition, funnel bubble collectors with an area of 0.03 m^2 were floated. ~~The a~~Auxiliary flux measurements from three lakes outside the study area w~~ere~~as conducted with the same method as for the OS lake. These measurements were utilised to assess the representativeness of the flux data collected on the MS and OS lakes.

The ~~CO_2 and CH_4~~ diffusive fluxes of CO_2 and CH_4 were calculated from the change in the CO_2 and CH_4 mixing ratios inside the closed chamber. The rate of change was calculated with linear regression based on ordinary least squares, similarly to the fen ecosystem chamber measurements by Heiskanen et al. (2021).

The measurement data of diffusive fluxes were screened to reject cases with non-linear concentration change and disturbances due to chamber leakage and ebullition events. The number of accepted/total data of the MS lake fluxes was 54/56 in 2017 and 62/75 in 2018. The number of accepted/total OS lake data was 42/50 for ~~of the OS lake~~ diffusive CO_2 fluxes ~~was 42/50~~ and 49/50 for diffusive CH_4 fluxes ~~49/50~~. There were ebullition events in 7 % of the individual flux measurements ~~on the OS lake~~ ~~in 2017.~~ and t~~T~~his ebullition frequency was used to estimate the total ebullition-induced flux over the ice-free period.

2.3 Abiotic and biotic environmental measurements

In addition to the C flux measurements, meteorological and environmental variables were measured continuously at and close to the flux measurement locations in the pine forest, fen, and lake ecosystems. Air temperature, precipitation sum and snow depth were measured at the weather station of the Finnish Meteorological Institute, located between the pine forest and fen EC measurement sites. Air temperature and humidity (Vaisala HMP 230), global and reflected radiation (Kipp&Zonen CM7), and

downward and upward PPFD (Kipp&Zonen PQS 1) were measured at the forest and fen sites at heights of 14 m and 3 m, respectively. Water vapour pressure deficit ~~(VPD)~~ was calculated from air temperature and relative humidity according to Jones (2013). Forest soil temperature ~~(T_s)~~ was measured at 5 and 10 cm depths (Onset, HOBO) and soil moisture at 10 cm depth (Onset, HOBO). T_s profiles at the fen were measured from a string (at 10, 30, 50, 75 and 105 cm depth) and flark (at 10, 30 and 50 cm depth) (IKES Pt100 sensors). The water table level (WTL) was measured manually from the flux chamber positions at the fen and OS lake, while the WTL of the MS lake was measured with a pressure sensor (Onset, HOBO U20) at the floating flux chamber position. Lake water temperature (Onset, HOBO Pedant) was measured at the same position at 10 cm from the lake bottom.

The ice-free period of the flux measurement lakes was determined from air temperature data and repeat digital photographs at the fen site (Linkosalmi et al., 2022). In October 2018, the lake freezing was recorded with a temperature and pressure logger (Onset, HOBO). The freezing occurred after air temperature remained continuously below 0 °C for three days with no subsequent exceedances. The timing of thaw was determined from the snowmelt and ice thaw at the fen.

We defined meteorological drought ~~on the basis of~~based on the atmospheric VPD as the period during which the daily maximum VPD (VPD_{max}) exceeded 20 hPa (Lindroth et al., 2007; Aurela et al., 2007).

The Standardised Precipitation Evapotranspiration Index (SPEI), which takes into account both precipitation and potential evapotranspiration in determining drought conditions (Vicente-Serrano et al., 2010), was used as a climatological reference for the study period. Monthly SPEI data covering the years 1950–2018 for the 0.5º × 0.5º grid cell including Kaamanen were extracted from the global SPEI database (SPEIbase v2.6, https://spei.csic.es/database.html, last access 19 October 2021).

2.4 Estimati~~onng~~ of pine bog flux~~es~~

In the subarctic aapa mires, pine bogs typically form narrow zones bordering forests and peatlands. Conducting direct EC flux measurements on them is challenging~~,~~ as the fetch is too limited for the EC method. Thus, the fluxes of the two pine bog ecosystems within the study area were not directly measured but, to enable regional upscaling, were modelled based on the fluxes measured in the forest and fen ecosystems. The use of forest and fen fluxes was considered appropriate because, first~~as~~ the tree species composition in pine forest and pine bog is similar and, second, the peat soil ground layer vegetation of pine bog is similar to that of the string top PCT at the fen (Table A1).

For estimating the pine bog fluxes, the total forest flux was assumed to consist of the flux of trees and the flux of the other forest ecosystem elements,

$$F_{\text{forest}} = F_{\text{forest,trees}} + F_{\text{forest,other}} \tag{2}$$

and similarly for the pine bog ecosystem:

$$F_{\text{pine bog}} = F_{\text{pine bog,trees}} + F_{\text{pine bog,other}}. \tag{3}$$

The 'trees' fluxes were assumed to be proportional to tree biomass, i.e.

$$F_{\text{pine bog,trees}} = a \times F_{\text{forest,trees}}, \tag{4}$$

14

where a is the tree biomass ratio between pine bog and pine forest (a = 0.52 and 0.16 for treed and sparsely treed pine bog, respectively; Table A54; see Sect. S.4 in the Supplement for biomass measurements and maps). Assuming further that the ground layer ('other') fluxes in both forest and pine bog equal the flux of the fen's driest PCT, i.e. string top,

$$F_{\text{forest,other}} = F_{\text{pine bog,other}} = F_{\text{string top}}, \tag{5}$$

Eqs. (2)–(5) show that the GPP and ER fluxes for the pine bog can be estimated as

$$F_{\text{pine bog}} = a \times F_{\text{forest}} + (1 - a) \times F_{\text{string top}}, \tag{6}$$

where F_{forest} and $F_{\text{string top}}$ are obtained from measurements.

2.5 Upscaling fluxes to landscape-level

The CO_2 and CH_4 fluxes of different ecosystems were upscaled to landscape-level by taking into account the areal contributions inside the 7 km^2 study area (Tables 1, A7) and summing the half-hourly area-weighted NEE, GPP, ER and CH_4 flux estimates of each ecosystem. The pine forest and pine bog daily average growing season CH_4 flux estimates were taken from literature (Bubier et al., 2005; Dinsmore et al., 2017), which were further calculated for 180 day long growing seasons at Kaamanen. The annual CO_2 and CH_4 balances for lakes were derived from the results of Kou et al. (2022), who modelled these fluxes for the Kaamanen catchment with the Arctic Lake Biochemistry Model (ALBM). ALBM is a one-dimensional process-based model operating on a daily time step (Tan et al., 2015, 2017). For Kaamanen, it was calibrated with the flux measurements described in Sect. 2.2.4 and driven with local meteorological data (Kou et al., 2022). The annual balances of the OS lake were estimated for the second study year from the previous year's measurements by scaling with the ice-free period length.

2.6 Estimating flux uncertainty

The uncertainty of the EC-based CO_2 and CH_4 fluxes of the pine forest and fen ecosystems were estimated by taking into account the most significant error sources. First, the uncertainty related to low turbulence screening was estimated by filtering the data with 100 bootstrapped u_* thresholds and gap-filling each of the resulting time series. The related uncertainty was defined as the standard deviation of the 100 gap-filled 30 min NEE values. Second, to estimate the random measurement uncertainty, we binned the measured data into 0.2 (pine forest) or 0.1 mg CO_2 m^{-2} s^{-1} (fen) wide bins and calculated the standard deviation of model residuals for each bin. The linear relationship between this standard deviation and the magnitude of the flux was estimated separately for negative and positive fluxes and used to estimate the uncertainty of measured data (Richardson et al., 2008). Third, the uncertainty due to gap-filling with XGBoost was estimated following the procedures detailed by Irvin et al. (2021). This uncertainty component was estimated from an ensemble of 10 models that were fitted using bootstrapped data and the uncertainty intervals were calibrated using Platt scaling as an additional post-processing step. To estimate the uncertainty of the annual balances, the uncertainty related to u_* was determined as the standard deviation of the 100 bootstrapped balances. Also, the gap-filling uncertainties were determined using a bootstrapping approach. For winter, we resampled the winter-time data 100 times with replacement and calculated alternative balances. For the growing season,

15

390 we used the ensemble of 10 XGBoost models to calculate alternative balances. In both cases, the gap-filling uncertainty was determined as the standard deviation of the balances.

~~The uncertainty of the EC-based CO_2 and CH_4 flux sums of the pine forest and fen ecosystems were estimated by taking into account the most significant error sources similarly to the method described in Heiskanen et al. (2021). The random error was estimated for the statistical measurement error and the error caused by gap-filling of missing data (Räsänen et al., 2017).~~

395 ~~Additionally, the annual error due to friction velocity filtering was estimated by recalculating the annual EC-based CO_2 and CH_4 balances with modified data sets that were screened with two additional friction velocity limits (pine forest: 0.19 and 0.31 m s^{-1}, fen: 0.05 and 0.15 m s^{-1}). This error was calculated as the average deviation from the annual balance calculated with the optimal friction velocity limit (pine forest: 0.24 m s^{-1}, fen: 0.1 m s^{-1}) (Aurela et al., 2002).~~

For the flux chamber-based monthly CO_2 and CH_4 flux sums of the lake ecosystem, the measurement uncertainty was estimated

400 ~~from~~ as the standard deviation of the flux data from the repeated chamber closures. The uncertainty of the annual CO_2, CH_4 and C flux sums were accumulated as the root sum square of individual uncertainties.

For the modelled pine bog fluxes, both for treed and sparsely treed bogs, the uncertainty was combined from the pine forest string top flux uncertainties proportionally to their contribution to the derived flux. The string top flux uncertainty was estimated by combining the uncertainty due to the estimated parameters of environmental response functions and the flux

405 variation among the chamber plots (Heiskanen et al., 2021).

The landscape-level flux uncertainty was calculated by combining the total uncertainties of each ecosystem, excluding lakes due to differing data set, proportionally to their areal coverages (Table 1). All uncertainty estimates reported for C balances refer to the 95 % confidence intervals.

2.7 Statistical analysis

410 The estimates of ~~monthly~~ ER, GPP, NEE and CH_4 fluxes~~exchange~~ of ~~each~~ pine forest and fen ecosystems were compared between the two growing seasons using ~~Welch's t test for the lake data, which comprised a sample of measured fluxes, and~~ the Z test ~~for the other ecosystems~~, for which we produced full flux time series with uncertainty estimates. Welch's t test was used for comparing the monthly average lake fluxes between the two years, as the compared data comprised of a sample of measured fluxes.

415 For identifying the main environmental drivers of the pine forest CO_2 flux, a linear regression model was estimated to explain the 5-day averaged GPP and ER fluxes derived from the measured EC data. The F_R data were normalised to 10 °C (denoted as F_{R10}), while the F_{GPP} data were normalised to a near-optimal PPFD level of 1200 µmol m^{-2} s^{-1} (denoted as $F_{GPP1200}$) (Laurila et al., 2001).

The following fixed explanatory 5-day variables were tested in the models: precipitation sum, average VPD_{max}, soil moisture

420 and temperature at a depth of 10 cm, air temperature and daily maximum PPFD. T_s was included in the final analysis while air temperature was excluded, because these variables were strongly correlated (Pearson's $R = 0.96$ in the F_R data and $R = 0.93$ in the $F_{GPP1200}$ data) and T_s showed higher absolute correlation with the response variables. The MODIS Normalised Difference

Vegetation Index was also tested as an explanatory variable, but it was excluded from the final analysis, as it strongly correlated with T_s (Pearson's $R = 0.87$ in the F_R data and $R = 0.89$ in the $F_{GPP1200}$ data). For the final models, the explanatory variables

425 were chosen with a stepwise procedure to both directions by minimising Akaike's information criterion value. To evaluate the relative impact of each explanatory variable, the standardised regression coefficients were calculated. Data analyses were conducted in R (R Core Team, 2021) with the ~~packages~~ MASS (Venables and Ripley, 2002) and MuMIN (Barton, 2020) packages.

3 Results and discussion

430 ### 3.1 Environmental conditions

We studied CO_2 and CH_4 fluxes across different ecosystem types in Kaamanen from June 2017 to June 2019. The growing seasons (May–October) of 2017 and 2018 differed from each other in terms of their meteorological conditions, which affected the CO_2 and CH_4 exchange between the atmosphere and ecosystems. The early growing season in 2017 was colder than the corresponding period in 1981–2010 on average (Pirinen et al., 2012), with May being 1.9 °C and June 1.4 °C colder (Fig. 3).

435 The summer months June–August were rainy in 2017, which was reflected in cloudiness that decreased the incoming solar radiation, with July in particular being cloudy (Fig. 4). In contrast, the spring of 2018 was warm, with May being 3.8 °C warmer than the 30-yr May average. In July 2018, a widespread drought and heatwave event in north-west Europe reached Kaamanen and caused the monthly mean air temperature to rise to 18.6 °C, which was 5.3 °C higher than the 30-yr July average. Additionally, the monthly precipitation sum was less than half of the 30-yr average (34 and 72 mm, respectively).

440 After the drought, the following August and September were also warmer than the corresponding 30-yr averages, by 1.5 and 1.9 °C, respectively, but precipitation sum was then double the 30-yr average. The spring 2019 was characterised by a dry and warm April (3.7 °C above the long-term average) and rainy weather in May and June. Lake water levels were visibly lower in 2018 exposing the shoreline sediments of shallow lakes, for instance in the MS lake of this study.

17
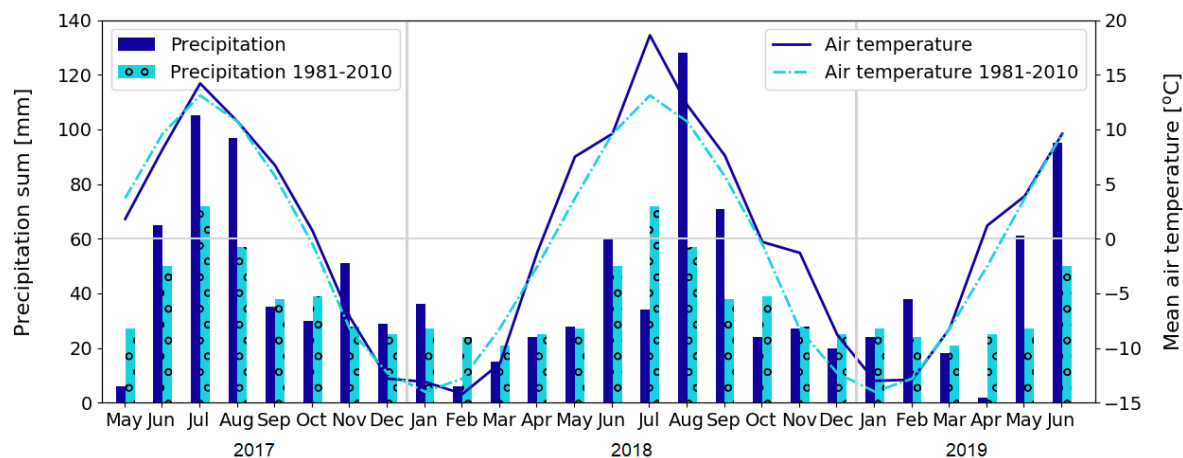
Figure 3. Monthly precipitation sum and mean air temperature at Kaamanen, and the corresponding 30 -yr averages (Pirinen et al., 2012) measured at the Ivalo weather station (68°36' N, 27°25' E; 59 km south of Kaamanen).
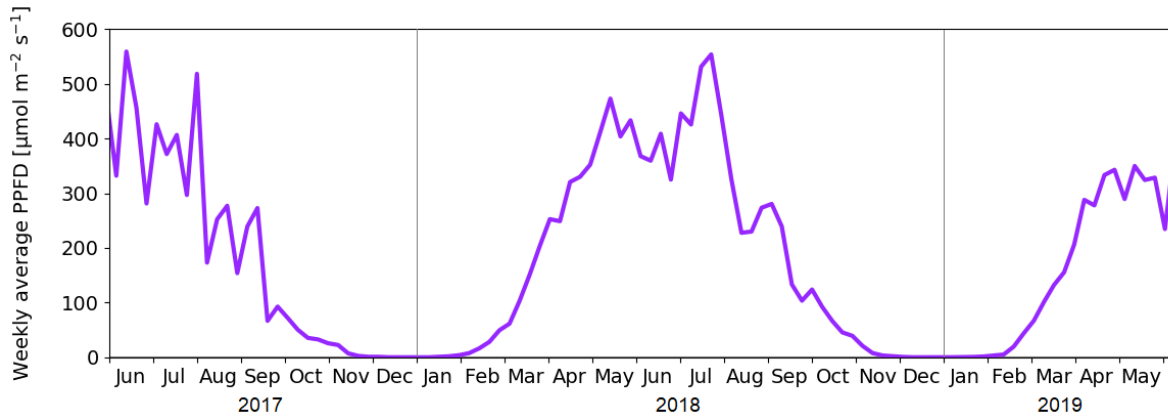

Figure 4. Weekly average photosynthetic photon flux density (PPFD) measured at Kaamanen.

The forest soil freeze and thaw occurred each year in the end of October and mid-May, respectively (Fig. 5a). In late autumn 2018, the forest T_s decreased from 8 °C to 1 °C in just 20 days between 23 September and 13 October, which was due to the lack of snow cover. In the fen, the surface peat of the strings froze concurrently with the forest soil (Fig. 5b). However, the thaw occurred slightly earlier in the strings than in the forest, where trees shaded the surface. The continuous water saturation in the flark peat led to weaker peat temperature responses to changing air temperature than in the dryer strings. The lake water temperature, measured only during the ice-free periods of 2017 and 2018 (Fig. 5c), was affected, in addition to air temperature, by the incoming flow to the lake and by the water level. Following the air temperatures, the forest soil, fen peat and lake water temperatures were higher in July 2018 than in 2017.

18
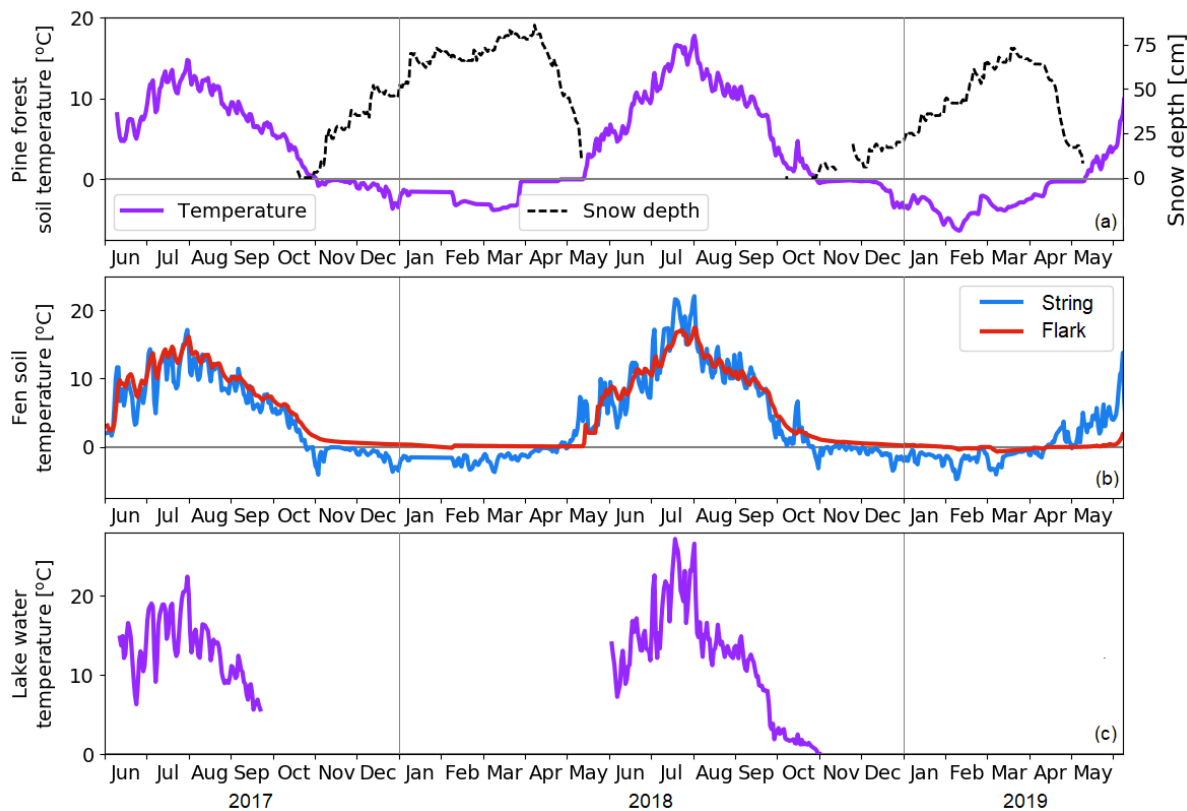
Figure 5. Daily average (a) forest soil temperature measured at 10 cm depth and snow depth, (b) fen peat temperature measured from strings and flarks at 10 cm depth and (c) MS lake water temperature at~~of~~ the floating chamber position 10 cm from the bottom.

460   The ice-free period of the measured lakes lasted for 167 and 176 days (from May to October) during the first and second study year, respectively (Table 4).

Table 4. Estimated ice-free period start and end dates of the studied lakes.

Period start	Period end
25 May 2017	26 October 2017
10 May 2018	30 October 2018
5 May 2019	19 October 2019

The meteorological drought lasted from 2 July to 1 August 2018 (Fig. 6a). The drought limit of daily $VPD_{max} \underset{=}{} 20$ hPa was

465   exceeded on 13 days in total in 2018, while no exceedances took place in 2017. The average daily maximum VPD in 2 July – 1 August 2018 was 16.9 hPa, while during the same period in 2017 it was 9.4 hPa. The corresponding daily air temperatures were 18.5 and 14.2 °C, respectively. The highest daily maximum VPD of 31 hPa was observed on 18 July 2018. VPD responded rapidly to the reduced amount of water in the environment, while the water table level in the fen, the water depth of lakes and the forest soil moisture decreased gradually as the drought developed (Fig. 6).

19

470   Within the fen, WTL varied strongly among the plant community types (Fig. 6b). In the flark and *Trichophorum* tussock PCTs, WTL was most of the time close to or at the peat surface, while in elevated strings it was deeper from the peat surface, fluctuating between -10 and -20 cm in string margins and between -30 and -70 cm in string tops. The drought decreased the WTL in all plant communities simultaneously, and by mid-August WTL had recovered to a normal level except for the string tops.

475   The water depth of the MS lake was within 30–40 cm (Fig. 6c) and it dropped in June–July 2018 to less than 20 cm in the centre of the lake. This drawdown was associated with a shoreline retreat of 6 to 8 m. However, after the first rainfall in 3–5 August, the water depth quickly reverted to the pre-drought level. Our field observations and visual interpretation of satellite and drone imagery suggest that the water level drop magnitude was uniform in the waterbodies within the study area.

The annual cycle of the soil moisture measured in the pine forest showed a low moisture content (< 0.1 $m^3 m^{-3}$) during winter

480   and fluctuations after the soil thaw (Fig. 6d). During both springs, the water availability in soil was at its maximum in 10–14 May due to melting snow. The drought during summer 2018 was clearly indicated by the soil moisture data that showed a drastic drop from 0.2 to 0.1 $m^3 m^{-3}$ between 23 June and 22 July. After the rainfall in the beginning of August, soil moisture rose in a few weeks to the average growing season level. Thus, even though the meteorological drought was already over in the beginning of August, the water availability to vegetation was not yet fully recovered.

485   In terms of the drought index (SPEI), the drought event in July 2018 was the eighth most severe drought in Kaamanen between January 1950 and December 2018 (Fig. 7). However, the drought event was relatively short, and the five-month SPEI between May and September was close to neutral.
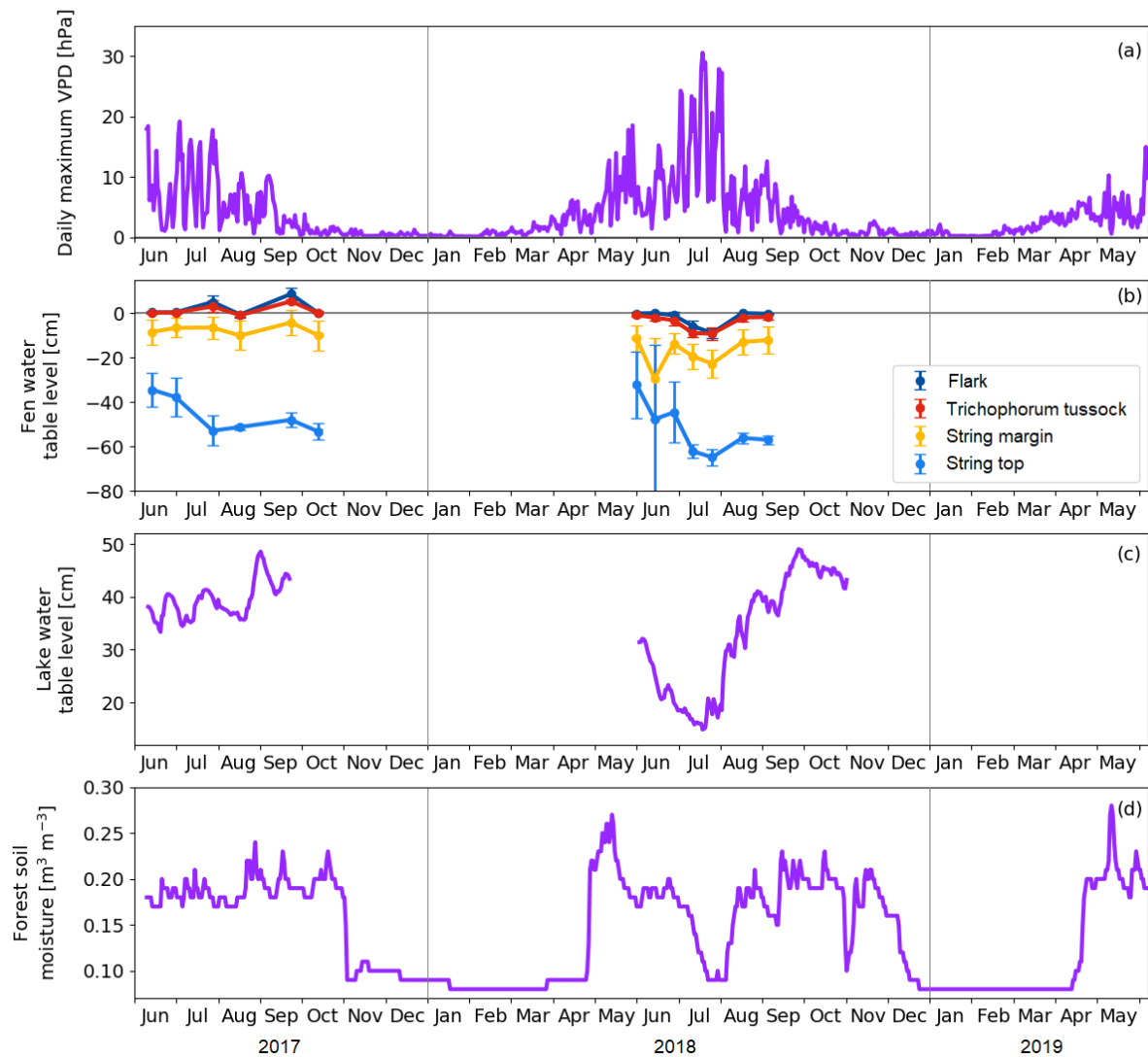
Figure 6. (a) Daily maximum vapour pressure deficit. (b) Mean water table level at the main plant communities of the fen. Error bars represent the standard deviation. (c) Water table level at the floating chamber position in Lake Jänkälampi. (d) Forest soil moisture at 10 cm depth.
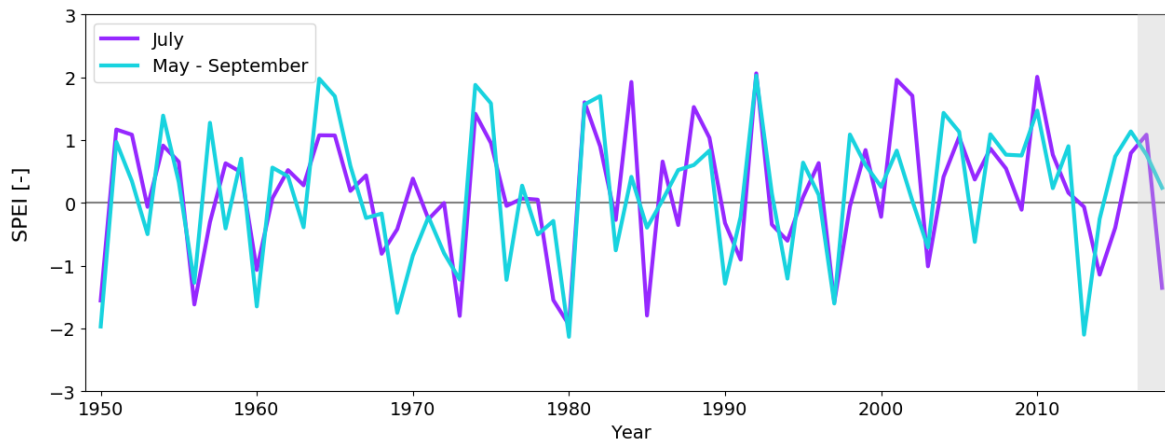
Figure 7. One month (July) and five-month (May-September) Standardised Precipitation Evapotranspiration Index (SPEI) ~~time series~~ at Kaamanen in 1950 – 2018. Positive SPEI values denote moist conditions and negative values drought conditions. Years 2017 and 2018 are marked with shading.

3.2 Ecosystem CO_2 and CH_4 fluxes

3.2.1 Pine forest fluxes

The pine forest acted as a net CO_2 sink during both study years. The annual CO_2 balances (with the 95% confidence intervals) during the first and second study year were -126 ± 21 and -101 ± 19 g C m^{-2}, respectively (Fig. 8b, Table A6). For other evergreen needleleaf forests in northern Fennoscandia, the observed balances have been smaller in magnitude: the Scots pine forest at Värriö in northern Finland was a CO_2 sink in 2012–2014 (-48 to -7 g C m^{-2}) and a small source in 2015 (14 g C m^{-2}) (Kulmala et al., 2019), while the Norway spruce forest at Kenttärova in northern Finland had a close-to-neutral balance (on average -2 g C m^{-2}) (Aurela et al., 2015).

There were two periods when the CO_2 fluxes behaved differently between the two study years due to differing meteorological conditions. First, even though the summer was warmer in 2018 than in 2017, and thus one could expect enhanced respiration, the ER fluxes of the pine forest ecosystem were on average similar during the growing seasons. This was due to the rainy period in June–August 2017 (Fig. 3), as a result of which forest soil remained saturated or nearly saturated in water during the whole growing season (Fig. 6d). As the forest soil moisture content was continuously close to the maximum water holding capacity, the effect of abundant precipitation emerged as increasing lake water table levels (Fig. 6c). We suspect that the stronger ER temperature response observed in June–August 2017 was caused by enhanced heterotrophic soil respiration (Fig. A1), which is known to increase with soil moisture until near water saturation (Orchard and Cook, 1983; Moyano et al., 2012; McElligott et al., 2017; Du et al., 2020).

The second period of dissimilar behaviour in CO_2 fluxes was observed when the drought and heatwave discussed above limited GPP fluxes; compared to the previous year, the GPP sum in 22 July – 17 August was 35 g C m^{-2} lower in 2018 (Z test, p = 0.003) (Fig. 8d). The daily maximum VPD surpassed the 20 hPa limit, indicating meteorological drought, for the first time on

22

2 July and the last time on 1 August 2018 (Fig. 6a), during which period the average air temperature was 5 °C higher than in the previous year (Fig. 3). In July 2018, the forest soil moisture at 10 cm depth also dropped by 50 % from the normal growing season level, decreasing to 0.1 $m^3\ m^{-3}$ on 22 July (Fig. 6d). Soil moisture recovered to a normal level three weeks later on 13 August.

520 ~~The pine forest acted as a net CO_2 sink during both study years. The annual CO_2 balances during the first and second study year were -78.3 ± 50.8 and -118.9 ± 26.8 g C m^{-2}, respectively (Fig. 8b, Table A5). Notably, the Kaamanen site is located about 150 km north to the other studied evergreen needleleaf forests in the region. Observations have shown that such forests in northern Fennoscandia region have acted as small annual CO_2 sinks (Aurela et al., 2015). The growing season (11 June – 31 October) GPP and ER sums were larger during the first measurement year than the second one (Table A6).~~

525 ~~There were three distinct periods during which the CO_2 fluxes diverged between the years, resulting in the difference in the annual balance. The first dissimilarity was that ER rates were larger during 15 June – 15 August 2017 compared to the same period in 2018 (Figs. 8c, A1). This was caused by the higher than average precipitation sum in 2017 (Fig. 3), which saturated or nearly saturated the soil with water throughout the peak growing season. As the forest soil moisture was continuously close to the maximum water holding capacity, the effect of abundant precipitation emerged as increasing lake water table levels (Fig.~~
530 ~~6c–d). We suspect that the higher ER in 2017 was caused by enhanced heterotrophic soil respiration, which is known to increase with soil moisture until near water saturation (Orchard and Cook, 1983; Moyano et al., 2012; McElligott et al., 2017; Du et al., 2020).~~

~~The second period of dissimilar CO_2 fluxes was observed when the drought and heatwave discussed above limited fluxes in 2018. Compared to the previous year, GPP was reduced in 22 July–17 August and ER in 26 July–15 August 2018 (Fig. 8c–d).~~
535 ~~The daily maximum VPD surpassed the 20 hPa limit, indicating meteorological drought, for the first time on 2 July and the last time on 1 August 2018 (Fig. 6a), during which period the average air temperature was 5 °C higher than in the previous year (Fig. 3). In July 2018, the forest soil moisture at 10 cm depth also dropped by 50 % from the normal growing season level, reaching 0.1 $m^3\ m^{-3}$ on 22 July (Fig. 6d). Soil moisture recovered to a normal level three weeks later on 13 August.~~

There is evident discrepancy between the timing of meteorological drought and reduced ecosystem CO_2 fluxes. The response
540 to drought in plants occurs both in roots, where water availability through soil is a key factor, and in the stomatal openings in leaves, where the gas exchange is affected by stomatal control due to VPD. The tighter stomatal control due to high VPD limits C assimilation (Martín-Gómez et al., 2017), and in Scots pine trees this has been estimated to occur at a VPD of 8 hPa while at approximately 28 hPa the stomata are fully closed (Büker et al., 2012). The drought seemed to have an effect on the CO_2 exchange until 18 August, even though soil moisture and VPD hardly had any direct effect anymore, as only after this date the
545 magnitude of ER and GPP fluxes were not continuously lower compared to the previous year. This lagged effect could be caused by embolism, defoliation or root degradation (Aguadé et al., 2015), or by weakened mycorrhizal symbiosis in the roots (Muilu-Mäkelä et al., 2015). Gao et al. (2017) also found that the GPP of a southern boreal Scots pine forest was suppressed during a severe soil moisture drought in the summer of 2006 as the plants regulated their stomata due to high VPD.

According to the linear regression model, the main environmental factors affecting the radiation-normalised GPP flux ($F_{GPP1200}$) of the pine forest were T_s, VPD_{max} and soil moisture (Table 5). The magnitude of $F_{GPP1200}$ increased with increasing T_s and soil moisture and decreased with increasing VPD_{max}. The positive correlation with soil moisture originated from the anomalously low moisture levels during the 2018 drought (Fig. 6d). The temperature-normalised respiration (F_{R10}) was affected by T_s, VPD_{max}, soil moisture and precipitation sum (Table 5). F_{R10} increased with increasing T_s, soil moisture and precipitation sum, and decreased with increasing VPD_{max}.
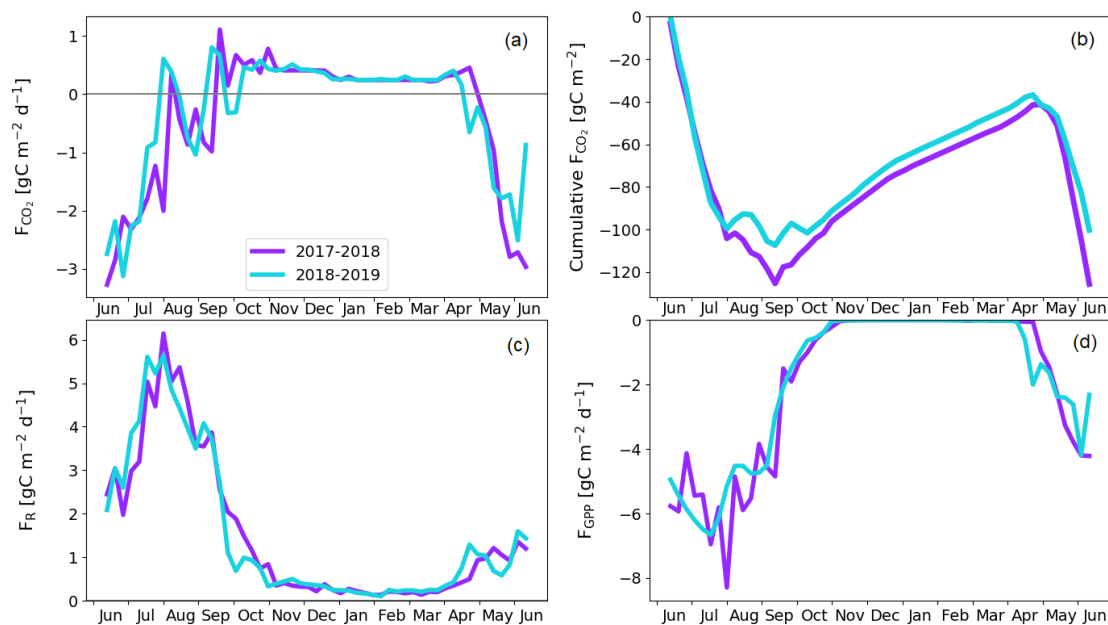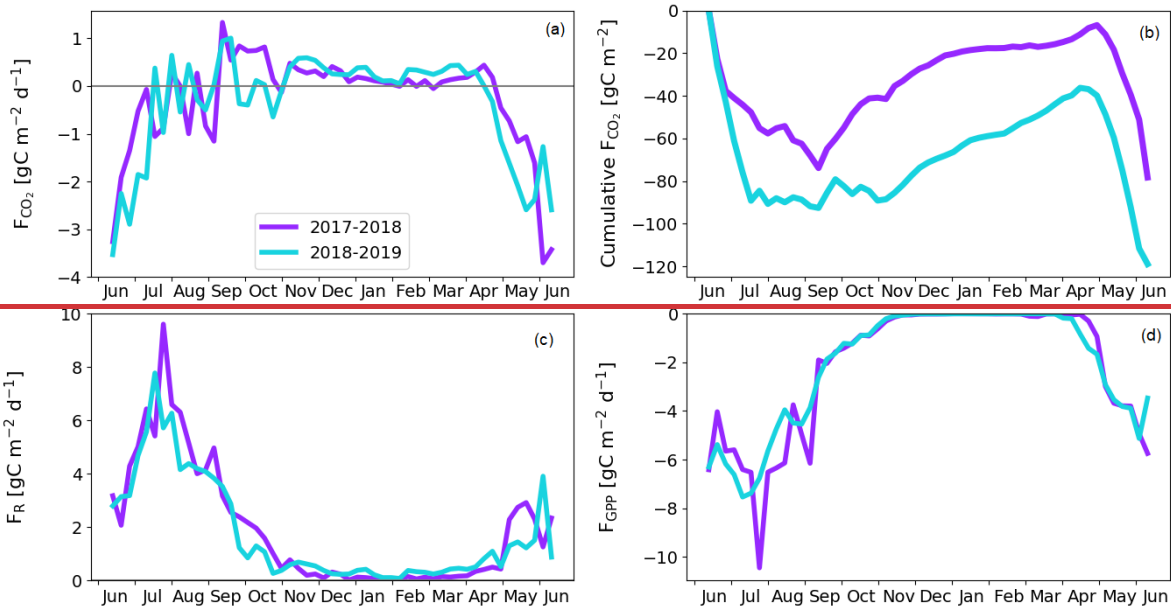
Figure 8. Pine forest gap-filled fluxes. Weekly averaged (a) and cumulative (b) CO_2 flux, and weekly averaged ecosystem respiration (c) and gross primary productivity (d).

Table 5: Standardised regression coefficients (± standard error) for the explanatory variables of the linear regression model for EC-based $F_{GPP1200}$ and F_{R10}. The adjusted coefficient of determination (R_a^2), normalised root mean square error (nRMSE; RMSE divided by the range of response variable values) and degrees of freedom (df) are also shown.

	Regression coefficient	df
$F_{GPP1200}$ ($R_a^2 = 0.78$, nRMSE = 0.12)		
T_s (-10 cm)	-1.02 ± 0.11	34
VPD_{max}	0.28 ± 0.11	34
Soil moisture (-10 cm)	-0.17 ± 0.08	34
F_{R10} ($R_a^2 = 0.68$, nRMSE = 0.15)		
T_s (-10 cm)	0.87 ± 0.18	31
VPD_{max}	-0.78 ± 0.18	31
Soil moisture (-10 cm)	0.24 ± 0.12	31
Precipitation sum	0.21 ± 0.11	31

3.2.2 Fen fluxes

The fen ecosystem was a small net CO_2 sink of -14 ± 17 g C m^{-2} and a small net CO_2 source of 9 ± 11 g C m^{-2} during the first and second year, respectively (Fig. 9b, Table A6). There were three periods during which either CO_2 or CH_4 fluxes diverged

25

570 between the years: the start of the growing season, the warmer-than-average growing season of 2018 and the drought and heatwave event in 2018.

The warm growing season increased the ER flux sum by 32 g C m^{-2} (Z test, $p = 0.124$) during 11 June – 23 September 2018 (mean air temperature 13.2 °C) compared to 2017 (10.5 °C). Half of this difference, 16 g C m^{-2} (Z test, $p = 0.043$), accumulated in just 26 days, 17 July – 12 August, when the temperature difference between the years was largest (13.4 °C and 17.9 °C in

575 2017 and 2018, respectively).

The earlier start of the growing season in 2018 resulted in a higher CO_2 uptake in 11–30 June compared to the previous year (Fig. 9, Table A6); the balances of this period were -5 ± 13 and -20 ± 17 g C m^{-2} in 2017 and 2018, respectively. This was due to the nearly doubled GPP (Z test, $p < 0.001$), which was 27 ± 3 and 49 ± 4 g C m^{-2} in 2017 and 2018, respectively. ~~The fen ecosystem was a net CO_2 sink during both study years. The annual CO_2 balance was 20.6 ± 3.6 and 7.6 ± 3.7 g C m^{-2} during~~

580 ~~the first and second year, respectively (Fig. 9b, Table A5). There were two periods during which the CO_2 fluxes diverged between the years: the start of the growing season and a drought and heatwave event in 2018.~~

~~The earlier start of the growing season in 2018 resulted in a higher CO_2 uptake in 11 30 June compared to the previous year (Fig. 9, Table A6); the balances were 4.8 ± 6.4 and 21.0 ± 10.1 g C m^{-2} in 2017 and 2018, respectively. This was due to the nearly doubled GPP, which was 27.6 ± 3.9 and 49.2 ± 7.3 g C m^{-2} in 2017 and 2018, respectively.~~ The increase of net CO_2

585 uptake in northern mires due to earlier snowmelt and warm spring temperatures has been reported previously by e.g. Aurela et al. (2004) and Sagerfors et al. (2008). The differences in CO_2 exchange between the microforms of the fen were studied in more detail by Heiskanen et al. (2021), who found that the magnitude of ER and GPP increased gradually from the wettest PCT, i.e., flark, to the driest one, i.e.~~,~~ string top. However, the variation in net CO_2 uptake among the microforms was weaker than in the two flux components. The increased GPP due to warm spring weather was observed in all main microforms.

590 However, the simultaneous increase in ER led to a significantly ($p < 0.05$) higher net CO_2 uptake only in string tops, when comparing the early growing seasons of 2017 and 2018 (Fig. A2).

The higher CO_2 uptake during the early growing season of 2018 was offset by the decreased uptake due to the drought and heatwave event in 8 July – 4 August 2018. The GPP sum was 17 g C m^{-2} smaller (Z test, $p = 0.229$) during this period in 2018 than in 2017 (Fig. 9d). ~~The higher CO_2 uptake during the early growing season of 2018 was offset by the decreased uptake due~~

595 ~~to the drought and heatwave event in 20 July 9 August 2018.~~ As discussed above, the drought was observed as higher-than-average temperatures (Fig. 3), an elevated VPD (Fig. 6a) and water level drawdown by 5–20 cm at the fen microforms (Fig. 6b). These anomalies likely caused drought stress in the mire plants (Alm et al., 1999). The drought stress reduced GPP and the high temperatures increased ER compared to the previous weeks and the same time period during the previous year (Fig. 9c,d). The CO_2 uptake decreased during this period, and at the end of the period the fen ecosystem even turned into a CO_2

600 source. Unlike the increased CO_2 uptake during the early growing season, which could be allocated largely to the string plant communities, the drought affected plant communities in all microforms (Heiskanen et al., 2021). The CO_2 exchange in flarks including *Trichophorum* tussocks was immediately affected by the lowering WTL in July and August 2018 (Fig. 6b), while the drier string communities were affected to a lesser extent.

26

While the fen was an annual net CO_2 sink it also acted as a CH_4 source to the atmosphere during both study years. The annual CH_4 balance was 7.8 ± 0.2 and 6.3 ± 0.3 g C m^{-2} during the first and second study year, respectively (Fig. 9f). ~~The annual CH_4 balance was 7.0 ± 0.2 and 6.3 ± 0.3 g C m^{-2} during the first and second study year, respectively (Fig. 9f).~~ The flark, *Trichophorum* tussock and string margin PCTs contributed 98 % of the emissions, with string margins accounting for 44 % of the emissions during the growing season of 2017 and all three having similar emissions in 2018 (Heiskanen et al., 2021).

The drought decreased the annual CH_4 emissions, mostly during 21 July – 28 August 2018, when the emissions were 0.8 g C m^{-2} lower (Z test, $p < 0.001$) than during the same period in the previous year (Fig. 9e). ~~The drought decreased the annual CH_4 emissions, mostly during 21 July – 28 August 2018, when the emissions were 0.8 g C m^{-2} lower than during the same period in the previous year (Fig. 9e).~~ Notably, the decrease in CH_4 emissions occurred a few weeks after the meteorological drought begun and continued well after the WTL had reverted to the pre-drought level. The decrease in CH_4 emissions is likely due to both reduced release of carbon compounds by plant roots and increased oxic soil zone, which reduced CH_4 production and increased CH_4 oxidation (Strack and Waddington, 2008; White et al., 2008; Deppe et al., 2010). The lagged recovery of CH_4 flux coinciding with the GPP recovery indicates the link between methanogenesis and plant root exudates. Unfortunately, the uncertainties of the monthly CH_4 balances derived from the manual chamber measurements were large and the lower emissions could not be allocated to any specific PCT. However, the CH_4 emissions from flarks were larger in 2018 than 2017, which suggests that the drought-induced decrease in emissions occurred for~~on~~ the *Trichophorum* tussock and string margin PCTs that had lower WTL (Fig. 6b) (Heiskanen et al., 2021). The drought, which covered large parts of north-western Europe, did not affect the CO_2 and CH_4 exchange at Kaamanen as much as it did at more southern mires, where the drought duration was longer, although the water level draw-down was similar in magnitude (Rinne et al., 2020).

The total carbon balance, i.e. the sum of the CO_2 and CH_4 fluxes, showed that the fen was an annual carbon sink of -7 ± 17 g C m^{-2} and a carbon source to the atmosphere, 15 ± 11 g C m^{-2}, in the first and second study year, respectively (Table A6). The lower net CO_2 uptake during the drought period contributed most of the difference between the years. ~~The total carbon balance, i.e. the sum of the CO_2 and CH_4 fluxes, showed that the fen was an annual carbon sink of -13.6 ± 3.6 g C m^{-2} and carbon neutral, -1.3 ± 3.7 g C m^{-2}, in the first and second study year, respectively (Table A5). The lower CO_2 uptake during the drought period contributed most of the difference between the years.~~ Previous studies at the Kaamanen fen show that the ecosystem has been on average a larger annual CO_2 sink,~~: -~~ -22 g C m^{-2} (from -4 to -53 g C m^{-2}) during 1997–2002 (Aurela et al., 2004), and a similar average annual CH_4 source,~~:~~ 6 g C m^{-2} in~~for~~ 1995, 1997–1998 and 2011–2016 (Hargreaves et al. 2001; Piilo et al., 2020).
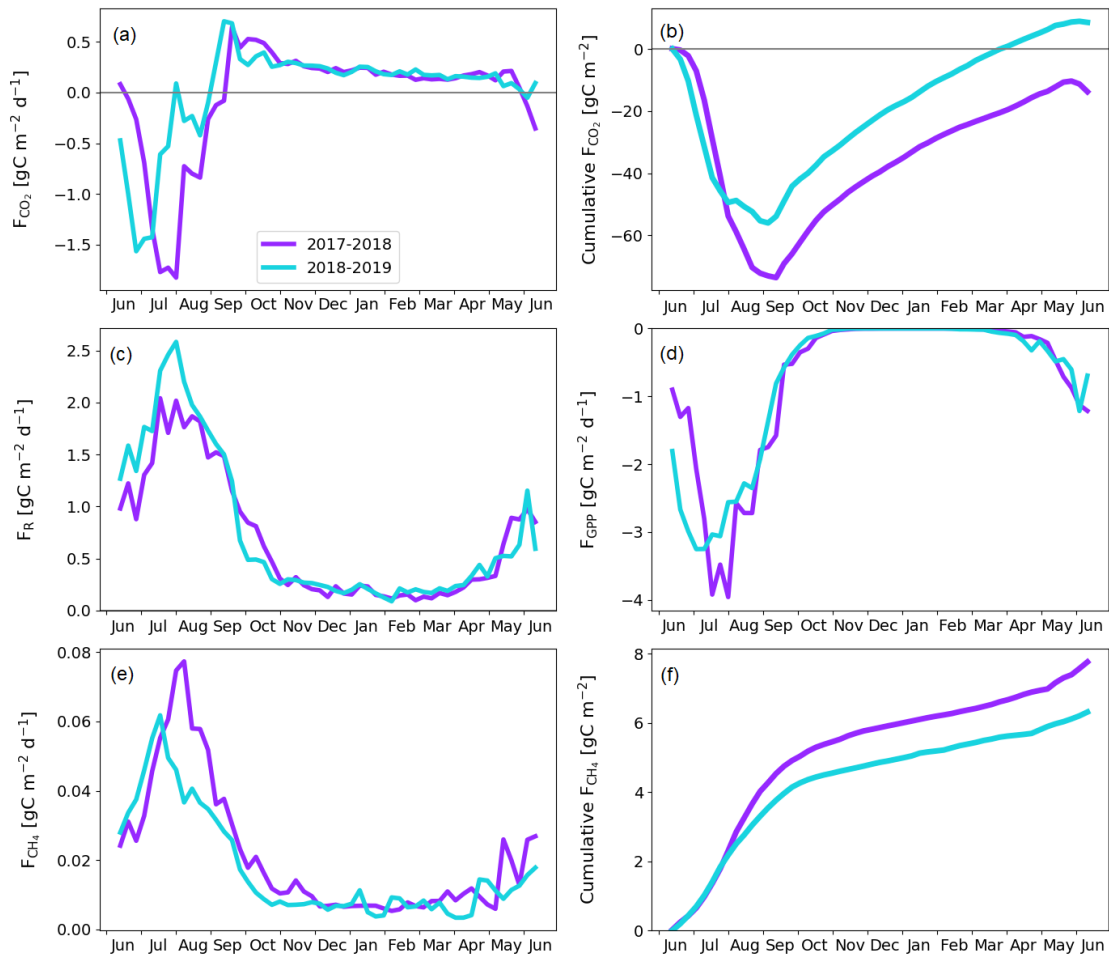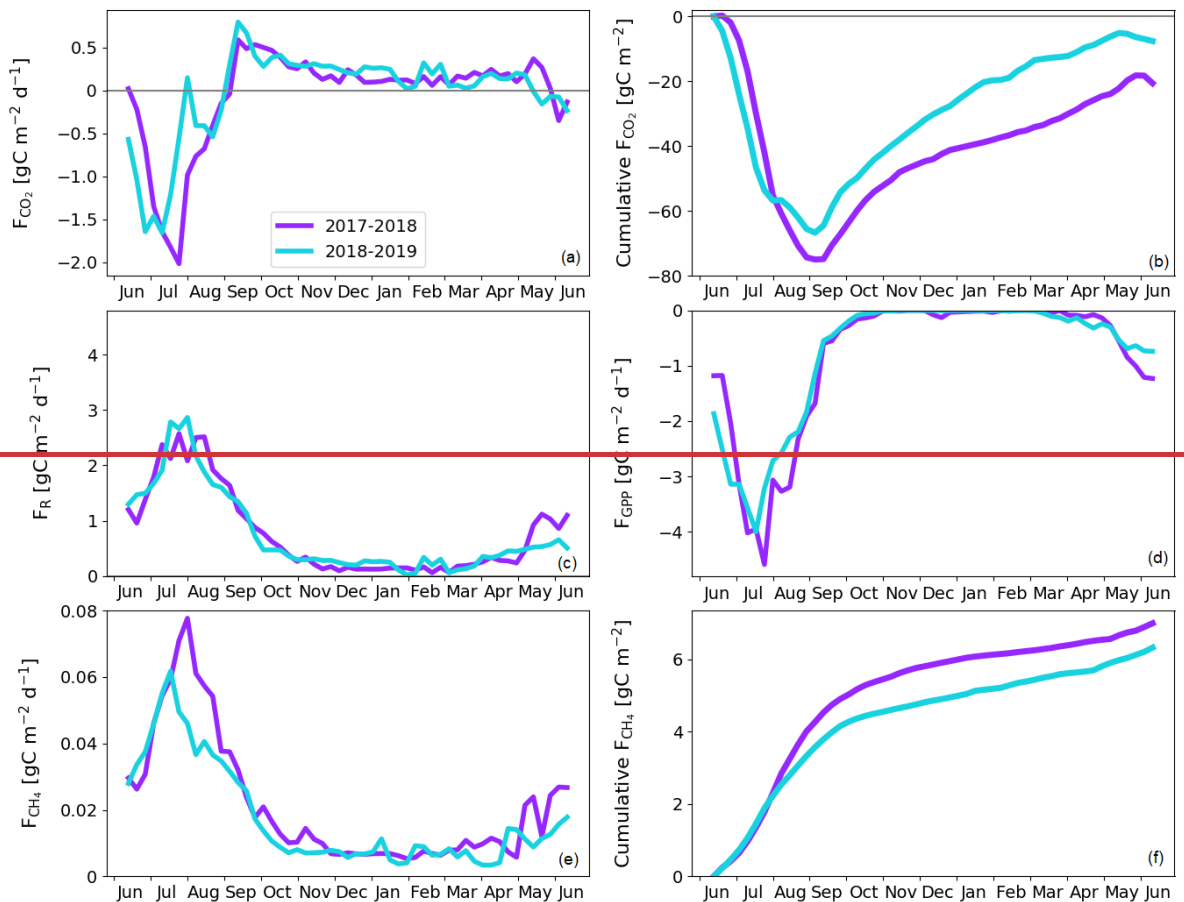
Figure 9. Fen gap-filled fluxes. Weekly averaged CO_2 (a), ER (c), GPP (d) and CH_4 (e) flux, and cumulative CO_2 (b) and CH_4 (f) flux.

3.2.3 Lake fluxes

The measured CO_2 fluxes of the OS and MS lake were on average 0.45 and 0.06 g C m^{-2} d^{-1} during the ice-free period, and the mean CH_4 fluxes were 0.014 and 0.003 g C m^{-2} d^{-1}, respectively (Fig. 10). The large difference in the flux rates between the lakes was most likely caused by the fact that the OS lake is situated immediately downstream from the fen (Fig. 1). Due to the location, the OS lake receives transported OC in the stream flow and has a higher lake water total organic C content than the MS lake (9 vs 5 mg L^{-1}) and a higher C content in its sediment (30.3 % C of dry mass) than in the MS lake sediment (5.5–22.6 % C, depending on location) (Table A8). Based on the ALBM model calculations (Kou et al., 2022), calibrated with the flux observations at the MS and OS lakes (Sect. 2.5), the annual CO_2 emissions were on average 28 g C m^{-2} from the MS lake and 97 g C m^{-2} from the OS lake. The modelled CH_4 emissions were 1.4 g C m^{-2} from the MS lake and 4.0 g C m^{-2} from the OS lake (Table 6).

The CO_2 emissions of the OS lake (0.2–0.8 g C m^{-2} d^{-1}) (Fig. 10a) were similar in magnitude, for instance, to those (0.3–1.4 g C m^{-2} d^{-1}) observed for Lake Stortjärn in Sweden, which is a northern boreal lake located adjacent to a mire (Denfeld et al.,

29

2020). In lakes with less organic carbon in water the net CO_2 emissions are lower, yet we did not observe CO_2 uptake by either of the studied lakes. In a similar shallow subarctic lake next to a fen at Abisko in Sweden, Jammet et al. (2017) found high CO_2 emissions of 33.3 g C m^{-2} during the spring period of 41 days, but photosynthetic CO_2 uptake during summer reduced the net emission of the ice-free period to 8.9 g C m^{-2}. Lohila et al. (2015) estimated an annual CO_2 balance of 33 g C m^{-2} for the shallow parts of the large subarctic Lake Pallasjärvi in Finland and recorded small CO_2 uptake during midday in the summer months. Also, small annual CO_2 emissions, 11.5 g C m^{-2}, were estimated for a small (9.6 ha) Lake Kipojärvi located near Kaamanen, surrounded by both an esker and a peatland (Juutinen et al., 2013). This shows that the CO_2 balance of lakes varies substantially from lake to lake in the subarctic region.

The annual CH_4 emissions of Lake Kipojärvi, 3.4 g C m^{-2}, were similar to the modelled OS lake emissions. The average daily diffusive CH_4 fluxes varied from 0.001 to 0.020 g C m^{-2} d^{-1} in this study and were similar to those reported in previous studies of boreal lakes. Denfeld et al. (2020) observed a range of 0.001–0.008 g C m^{-2} d^{-1} for Lake Stortjärn during the ice-free period, while Rasilo et al. (2014) found spatially highly variable CH_4 diffusive fluxes of 0.008 ± 0.020 g C m^{-2} d^{-1} across 224 boreal lakes in Canada during summer. The length of the ice-free period can considerably affect the annual emission of different boreal lakes as ice cover prevents gas exchange with the atmosphere (Guo et al., 2020).

Our estimate of ebullition was 22 % of the total CH_4 emission. This is smaller than observed in other studies of boreal lakes, especially considering that our study lakes are mostly shallow (< 2 m deep) and thus likely to show more frequent CH_4 ebullition than deep lakes (Bastviken et al., 2004). Contributions of 40–80 % of the total CH_4 emissions have been estimated for subarctic lakes (Bastviken et al., 2004; Wik et al., 2013; Jansen et al., 2020), and the annual CH_4 emissions of 1.0–8.3 g C m^{-2} have been observed (Bastviken et al., 2004; Thornton et al., 2015; Jammet et al., 2017). In general, there is high temporal and spatial variation in ebullition as there are both seep and non-seep areas where CH_4 bubbles emerge at the lake bottom, which complicates the ebullition estimation (Walter et al., 2006). Wik et al. (2018) found that the spatial ebullition potential was affected by the coarse detritus, buried aquatic vegetation and redeposited peat rather than the amount of total organic carbon or CH_4 in the sediment.

Both lakes showed the largest CO_2 emissions in early June (Fig. 10a). However, a similar development of fluxes was not observed with CH_4 (Fig. 10b). The dissimilarity between the gases is likely due to the differing production and accumulation processes. CO_2 emissions are driven by the amount of incoming dissolved and particulate carbon and the rate of decomposition of that organic carbon (Kortelainen et al., 2006), while CH_4 production is controlled by the substrates available for the methanogens to reduce it to CH_4 in anoxic conditions in sediments (Chapin et al., 2011). CH_4 concentration has been observed to be roughly constant with depth during the early summer, while CO_2 is strongly stratified, with a larger concentration towards the bottom of the lake (Denfeld et al., 2020). The breakdown of thermal stratification and turnover mixing occurs around the start and end of the ice-free period (e.g. López Bellido et al., 2009). At the MS lake, the flux measurements covered also the autumn turnover mixing in September, when CO_2 emissions increased compared to the previous month. The daily average CO_2 flux on the MS lake was lower in July 2018 than in 2017 (Welch's t test, $p = 0.01$) (Fig. 10), but no significant changes were observed in the measured CH_4 fluxes between the years.

Both lake types emitted 96 % of the total C efflux as CO_2 (Table 6). For comparison, in an extensive study of Alaskan subarctic lakes, the non-yedoma lakes emitted about 85 % as CO_2 and 15 % as CH_4 (Sepulveda-Jauregui et al., 2015), and in the above-mentioned 224-lake study the CH_4 diffusive fluxes contributed 8 ± 23 % to the total lake C emissions (Rasilo et al., 2014). The annual CO_2 and CH_4 balances of the study lakes were estimated from the fluxes measured during the ice-free period assuming no flux in winter. During the first study year starting on 11 June 2017, the lakes were free of ice in 11 June – 26 October 2017 and 10 May – 10 June 2018 and during the second year in 11 June – 30 October 2018 and 5 May – 10 June 2019 (Table 4). The C fluxes were measured during both years only on the mineral sediment (MS) lake, while the second year balances of the organic sediment (OS) lake, needed for landscape-level upscaling, were estimated from the first year's measurements. The estimated CO_2 emissions were 11.1 ± 3.5 and 14.2 ± 2.0 g C m^{-2} from the MS lake during the first and second ice-free period, respectively, and 74.7 ± 28.4 g C m^{-2} from the OS lake during the first year. This can be explained by the fact that the OS lake is situated immediately downstream from the fen (Fig. 1), and thus has a higher C content in the sediment (30.3 % C of dry mass) than in the MS lake (5.5 – 22.6 % C of dry mass, depending on location) (Table A7) and receiving the transported OC in the stream flow.

Both lakes showed largest CO_2 emissions in early June, right after the thaw (Fig. 10a), which were likely associated with the turnover caused by the break-down of thermal stratification. At the MS lake, the flux measurements covered also the autumn turnover mixing in September, when CO_2 emissions increased compared to the previous month. While the CO_2 emissions were influenced by the turnover mixing, a similar effect was not observed for CH_4 on either of the lakes. The daily CO_2 emissions of the OS lake (0.2–0.8 g C m^{-2} d^{-1}) were similar in magnitude, for instance, to those (0.3–1.4 g C m^{-2} d^{-1}) observed for Lake Stortjärn in Krycklan, Sweden, which is a northern boreal lake and also adjacent to a mire (Denfeld et al., 2020). In a similar shallow subarctic lake next to a fen at Abisko, Jammet et al. (2017) found high CO_2 emissions of 33.3 g C m^{-2} during the spring period of 41 days, but photosynthesis during summer reduced the net emission of the ice-free period to 8.9 g C m^{-2}. Lohila et al. (2015) estimated an annual CO_2 balance of 33 g C m^{-2} for the shallow parts of the large subarctic Lake Pallasjärvi and recorded small CO_2 uptake during midday in the summer months. This shows that the CO_2 balance of lakes varies substantially from lake to lake in the subarctic region. In Kaamanen, we did not observe notable CO_2 uptake by either of the lakes studied.

The annual CH_4 emissions through diffusive flux were 0.4 ± 0.2 and 0.7 ± 0.2 g C m^{-2} from the MS lake during the first and second ice-free period, respectively, and 2.4 ± 0.2 g C m^{-2} from the OS lake during the first year. We estimated that the CH_4 emissions through ebullition were 0.7 ± 0.2 g C m^{-2} from the OS lake during the first year and 0.1 ± 0.1 and 0.2 ± 0.1 from the MS lake during the first and second ice-free period, respectively. On the MS lake the CH_4 emission were higher in September 2018 than 2017 (Fig. 10b), likely due to warmer sediments and lower WTL (Figs. 5c, 6c).

The average daily diffusive CH_4 fluxes in Kaamanen (OS lake 0.014 g C m^{-2} d^{-1}, MS lake 0.003 g C m^{-2} d^{-1}) were similar to those reported in previous studies of boreal lakes (Fig. 10). Denfeld et al. (2020) observed a range of 0.001–0.008 g C m^{-2} d^{-1} for Lake Stortjärn during the open-water period, while Rasilo et al. (2014) found spatially highly variable CH_4 diffusive fluxes of 0.008 ± 0.020 g C m^{-2} d^{-1} across 224 boreal lakes in Canada during summer.

31

715 Our estimate of ebullition was 21 % of the total CH_4 emission from the Kaamanen lakes. Ebullition has been estimated to contribute 40–80 % of the total CH_4 emissions from open subarctic lakes (Bastviken et al., 2004; Wik et al., 2013; Jansen et al., 2020). The magnitude of annual CH_4 emissions of these lakes was 1.0–8.3 g C m^{-2} (Bastviken et al., 2004; Thornton et al., 2015; Jammet et al., 2017, to which range the Kaamanen lakes fall (OS lake 3.1 g C m^{-2}, MS lake 0.5–0.8 g C m^{-2}).

The estimated ebullition percentage of total emissions of Kaamanen lakes is conservative when comparing to other studies of boreal lakes, considering that the lakes in the Kaamanen area are mostly shallow (< 2 m deep) and thus likely to show more

720 frequent CH_4 ebullition than deep lakes (Bastviken et al., 2004). In general, there is high temporal and spatial variation in ebullition as there are seep and non-seep areas where CH_4 bubbles emerge at the lake bottom, which complicates the ebullition estimation (Walter et al., 2006). Wik et al. (2018) found that the spatial ebullition potential was affected by the coarse detritus, buried aquatic vegetation and redeposited peat rather than the amount of total organic carbon or CH_4 in the sediment. The OS lake in our study had five times as much C as the MS lake (Table A7) and a layer of redeposited peat, which led to sevenfold

725 CH_4 emissions compared to the MS lake.

The water level of the lakes decreased by about 15 cm during June–July 2018 as a result of drought and recovered to a normal level, similar to in 2017, quickly after the first rainfall in August (Fig. 6c), which changes could have affected the C fluxes. The monthly CO_2 flux on the MS lake was lower in July 2018 than in 2017 ($p = 0.01$), but no significant changes were observed in the CH_4 fluxes during the drought period.

730 Both lake types emitted 96 % of the total C efflux as CO_2 (Table 6). For comparison, in an extensive study of Alaskan subarctic lakes, the non-yedoma lakes emitted about 85 % as CO_2 and 15 % as CH_4 (Sepulveda-Jauregui et al., 2015), and in the above-mentioned 224-lake study the CH_4 diffusive fluxes contributed 8 ± 23 % to the total lake C emissions (Rasilo et al., 2014). The MS lake emissions (Table 6) were very similar to those from Lake Kipojärvi, a nearby small (9.6 ha) lake surrounded by an esker and a peatland, for which an annual balance of 15 g C m^{-2} has been determined (Juutinen et al., 2013).
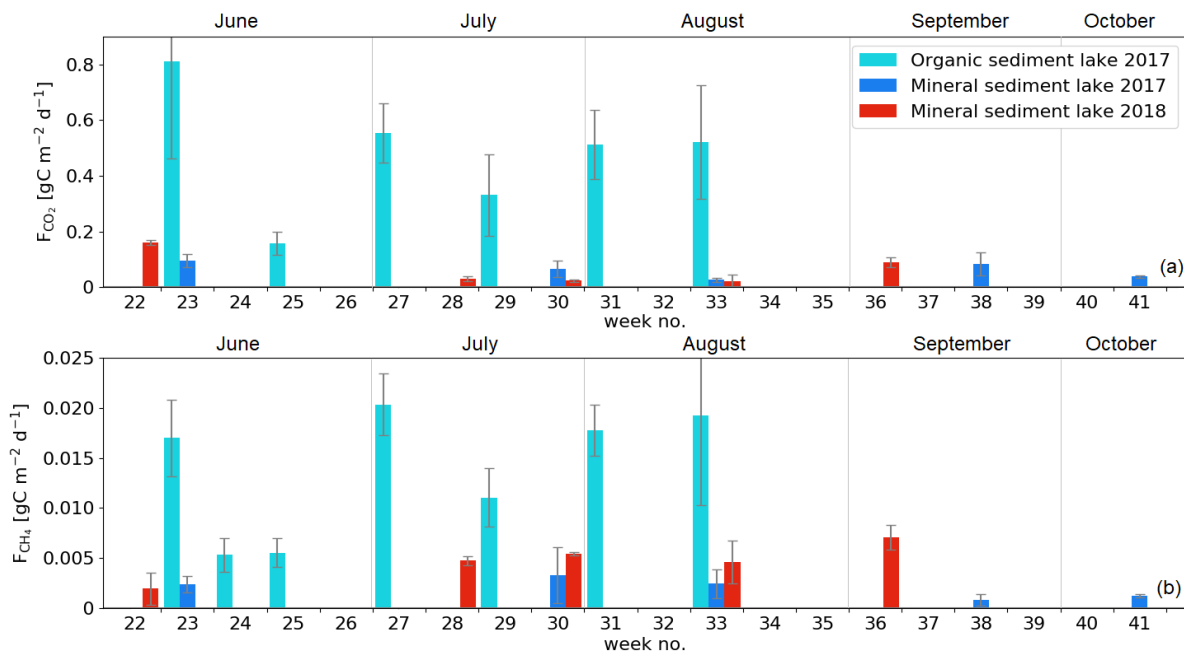
Figure 10. Weekly average lake CO_2 (a) and CH_4 (b) diffusive fluxes. Error bars represent the standard deviation of individual chamber measurements in each week.

Table 6. Modelled annual CO_2 and CH_4 balances [g C m^{-2}] of the MS and OS lakes during the two study years (Kou et al., 2022).

	11 June 2017 – 10 June 2018	11 June 2018 – 10 June 2019
Mineral sediment lake		
CO_2 flux	24.4	32.0
CH_4 diffusive flux	1.0	1.1
CH_4 ebullition flux	0.3	0.3
Total C flux	25.6	33.4
Organic sediment lake		
CO_2 flux	99.4	94.2
CH_4 diffusive flux	2.9	3.3
CH_4 ebullition flux	0.8	0.9
Total C flux	103.1	98.4

Table 6. Estimated CO_2 and CH_4 fluxes [g C m^{-2}] of the MS and OS lakes and during the ice-free periods within the study years.

	11 June – 26 October 2017 & 10 May – 10 June 2018	11 June – 30 October 2018 & 5 May – 10 June 2019
Mineral sediment lake		
CO_2 flux	11.1 ± 3.5	14.2 ± 2.0
CH_4 diffusive flux	0.36 ± 0.20	0.65 ± 0.20

33

CH$_4$ ebullition flux	0.10 ± 0.06 [a]	0.18 ± 0.06 [a]
Total C flux	11.6 ± 3.5	15.0 ± 2.0
Organic sediment lake		
CO$_2$ flux	74.7 ± 28.4	
CH$_4$ diffusive flux	2.44 ± 0.16	
CCH$_4$H$_4$ ebullition flux	0.66 ± 0.16	
Total C flux	77.8 ± 28.4	

[a] Estimated from the ratio between CH$_4$ diffusive and ebullition fluxes of the organic sediment lake.

3.2.4 Pine bog fluxes

The treed pine bog ecosystem between the forest and fen ecosystems covers 9.1 % of the studied landscape, and the sparsely treed pine bog covers 13.5 % and is located within the fen ecosystem in the driest parts of peatland. The annual CO$_2$ balance of the treed pine bog ecosystem was similar in the first and second study year, -92 ± 102 and -92 ± 110 g C m^{-2}, respectively (Fig. 11b, Table A6). The corresponding estimates for the sparsely treed pine bog ecosystem were lower and more uncertain: -48 ± 134 and -68 ± 145 g C m^{-2} (Fig. 12b, Table A6). The annual CO$_2$ balance of the treed pine bog ecosystem in the first and second study CO$_2$year was -39.1 ± 107.6 and -75.0 ± 111.2 g C m^{-2}, respectively (Fig. 11b, Table A5). While the annual CO$_2$ balance of sparsely treed pine bog ecosystem in the first and second study years was -9.8 ± 135.4 and -42.1 ± 145.3 g C m^{-2}, respectively (Fig. 12b, Table A5). The larger uncertainties of these balances compared to the forest and fen ecosystems were due to the contribution of the modelled string top fluxes, which were based on a limited number of chamber measurements (Sect. 2.4).

For both pine bog ecosystems, the GPP rates were higher during the latter year from mid-June to mid-July (Figs. 11d, 12d). For both pine bog ecosystems, from mid-June to mid-July, the ER rates were slightly lower in 2018 than in 2017 (Figs. 11c, 12c), and at the same time the GPP rates were higher during the latter year (Figs. 11d, 12d). This led to larger net CO$_2$ uptake during the first part of growing season in 2018 than in 2017 (Figs. 11a,b, 12a,b, Table A6). However, this difference in fluxes was more prominent in the sparsely treed pine bog. The drought event decreased the magnitude of GPP rate similarly in both ecosystems between mid-July and mid-August 2018 to a lower level compared to the previous two summer months and the same period in 2017 (Figs. 11d, 12d, Table A6).

The pine bog ecosystem fluxes were derived from the pine forest and fen ecosystem fluxes. String tops, which were used as a proxy for a treeless pine bog, are relatively dry microsites with a typical water table depth of 40–60 cm (Fig. 6b). As part of the bog ecosystems are wetter than typical string tops, and as the flark PCTs at Kaamanen had lower CO$_2$ fluxes than the string tops (Heiskanen et al., 2021), the proxy approach may bias the pine bog flux estimates. However, the use of string margin fluxes instead of the string top fluxes would not make any significant difference. The fluxes of the pine bog ground layer have been studied previously within a nearby Kipojärvi catchment by Juutinen et al. (2013), who found that in 2006 the ground layer was an annual CO$_2$ sink of -130 ± 91 g C m^{-2}, with an annual GPP sum of -456 ± 77 g C m^{-2} and ER sum of 326 ± 48 g

C m^{-2}. The ER sum was similar to that measured at the Kaamanen fen on the string top and margin PCTs (Heiskanen et al., 2021), but the magnitude of GPP sum ~~and thus the CO$_2$ sink were~~was greater for the Kipojärvi catchment~~, which led to the annual CO$_2$ sink being smaller than for the Kipojärvi catchment~~ (Fig. A2b). This suggest~~s~~ that our pine bog flux ~~model results~~estimates might underestimate the ~~ecosystem~~ true CO$_2$ sink of this ecosystem.
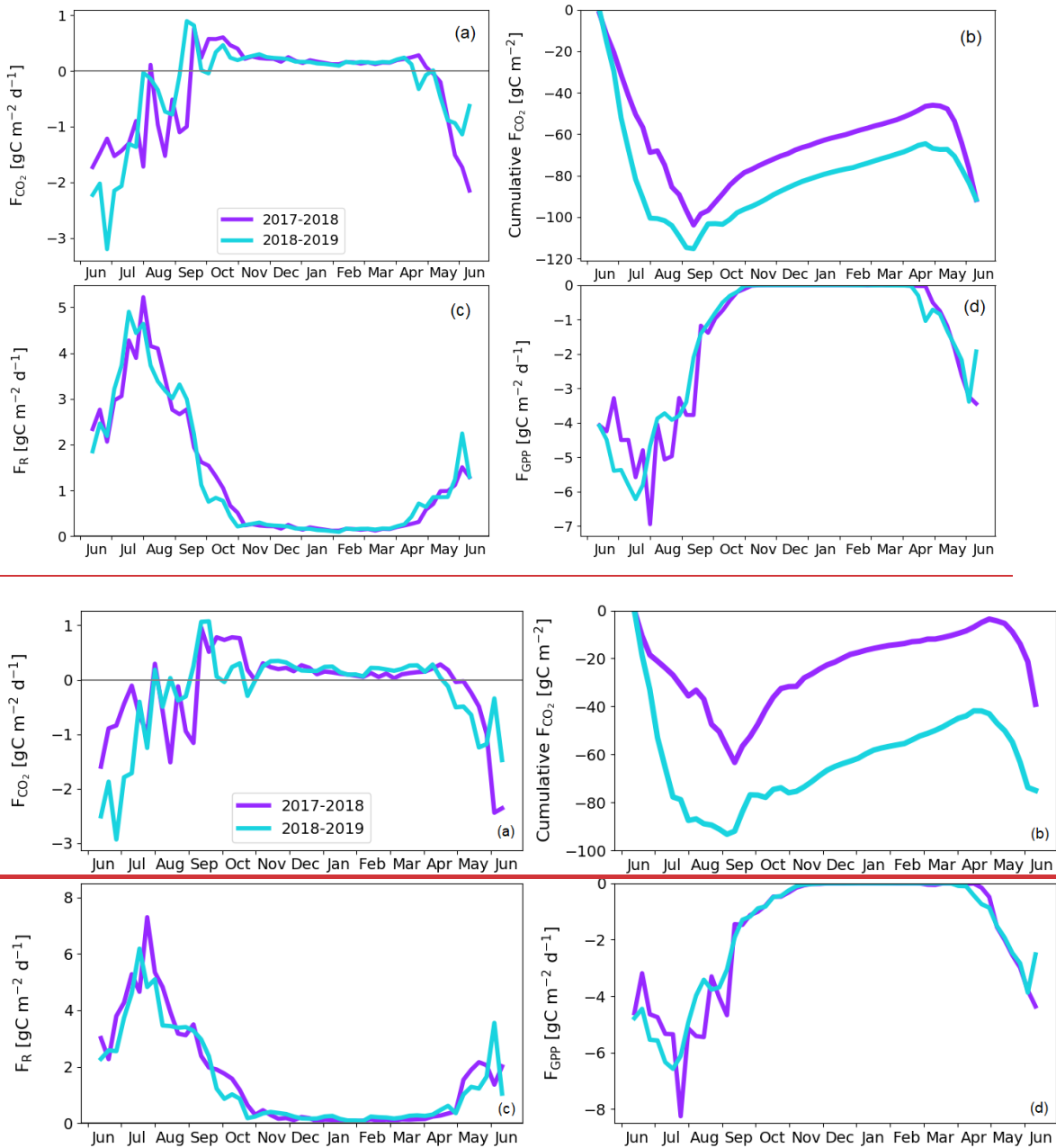

Figure 11. Treed pine bog gap-filled fluxes. Weekly averaged CO$_2$ flux (a), and cumulative CO$_2$ flux (b), and weekly averaged ER (c) and GPP (d) flux.
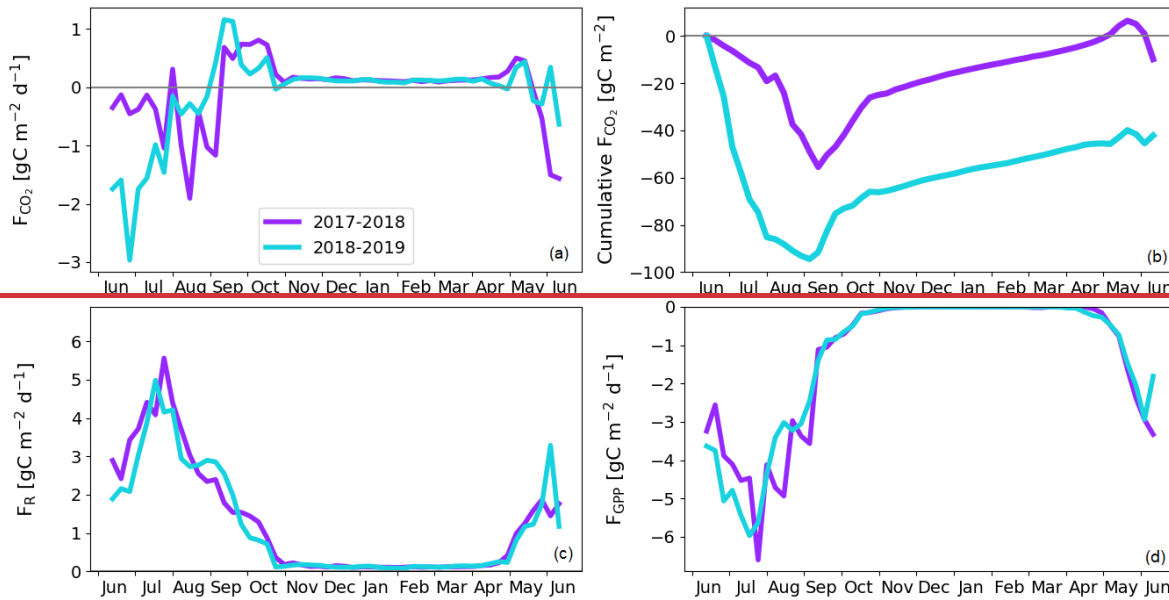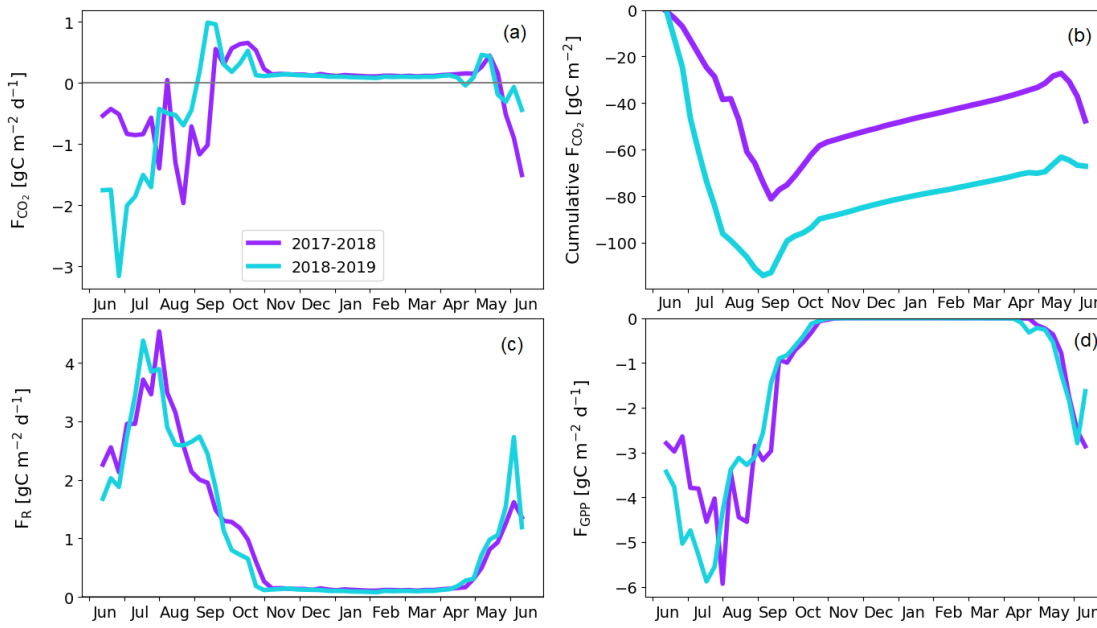
Figure 12. Sparsely treed pine bog gap-filled fluxes. Weekly averaged CO_2 flux (a), and cumulative CO_2 flux (b), and weekly averaged ER (c) and GPP (d) flux.

3.3 Upscaled landscape-level fluxes

By upscaling the ecosystem balances to our study area of 7 km², we obtained an annual landscape-wide CO_2 balance of -45 ± 22 and -33 ± 23 g C m² for the two study years. The corresponding CH_4 balances were 3.0 ± 0.2 and 2.7 ± 0.2 g C m², and

36

the sum of CO_2 and CH_4 balances were -42 ± 22 and -31 ± 23 g C m^{-2}, respectively (Fig. 13 b,f, Table A6). ~~By upscaling the ecosystem balances to our study area of 7 km², we obtained an annual landscape CO_2 balance of -25.9 ± 65.7 and -41.3 ± 64.9 g C m^{-2} for the two study years. The corresponding CH_4 balances were 2.4 ± 0.7 and 2.3 ± 0.7 g C m^{-2}, and the total C balances were -23.5 ± 65.7 and -39.0 ± 64.9 g C m^{-2}, respectively (Fig. 13 b,f, Table A5).~~ The pine forest ecosystem contributed to the total landscape C balance with a large CO_2 sink and a minimal CH_4 sink. In the evergreen forest ecosystem, CO_2 uptake period was longer than that of the fen ecosystem~~.~~, by 12 days at~~in~~ the beginning of the growing season and by 30 days at the end of the growing season (Figs. 8d, 9d), and during the first half of growing season the magnitude of CO_2 uptake was larger in the forest (Figs. 8a, 9a). The lake ecosystem was a complete opposite with substantial CO_2 and CH_4 emissions, while the fen ecosystem balances were between forest and lake with annual net CO_2 uptake and CH_4 emissions, although the fen had larger CH_4 emissions per unit area than the lake~~s ecosystem~~. The pine bog ecosystems, which were modelled using pine forest and fen fluxes, most likely acted as CO_2 sinks and CH_4 sources. The ~~magnitude of~~ ecosystem-specific CH_4 emissions w~~ere~~as much ~~smaller~~ lower than the magnitude of CO_2 exchange, with the exception of the fen ecosystem. The fen CH_4 fluxes largely determined the landscape-level CH_4 emissions (Fig. 14). The average annual terrestrial C uptake of the landscape was 338 ± 156 t C, of which 24 % was released back to the atmosphere by the lakes, resulting in a net C uptake of 256 ± 156 t C within the landscape (Fig. 14). ~~The average annual C uptake of the landscape was -274 ± 169 t C of which 20 % (55 ± 16 t C) was released back to the atmosphere by the lakes (Fig. 14).~~

The studied landscape consisted of roughly an~~d~~ equal area of pine forest, pine bog, open peatland and lakes (Table 1). Kou et al. (2022) studied the effect of land cover type misclassification to ecosystem and landscape C balances at Kaamanen using biogeochemical and atmospheric models. Their study area encompassed the entire 32.8 km² catchment at Kaamanen. In relation the 7 km² area of this study partially coincided with the most southern part of the catchment. The catchment consisted of proportionally more pine forest (53 %) and less open peatland (16 %), lakes (13 %) and pine bogs (9 %). In contrast to this study, birch dominated ecosystems (1 %) and mixed forests (6 %) were also present in the area. Thus, the 7 km² study area represented almost all ecosystems found in the greater landscape area around Kaamanen. The average annual landscape CO_2 balance was -104 g C m^{-2} and CH_4 balance 2.4 g C m^{-2}. The larger annual landscape CO_2 uptake on catchment-scale highlights the effect of proportionally larger forested area that were effective in CO_2 sequestering. Aurela et al. (2015) estimated an annual landscape-level CO_2 balance of -5 g C m^{-2} for a 1963 km² area in Pallas in north-western Finland that was comprised of 71 % pine forest, 12 % open wetland, 6 % water surfaces and 2 % treeless fell tops. Within this area, the 105 km² Lake Pallasjärvi catchment that included less forests and peatlands, but more lake and fell area, the annual landscape-level CO_2 balance was estimated to be 15 g C m^{-2}. The annual CO_2 uptake in Pallas was lower than in Kaamanen in spite of the much larger proportion of forests. In a study temporally overlapping our study, Chi et al. (2020) reported landscape-level C balances for a typical northern boreal forest landscape in Svartberget, Sweden, where forests covered 87 % of the area; the annual landscape-level CO_2 balance was -37 g C m^{-2} in October 2016 – September 2017 and -108 g C m^{-2} in October 2017 – September 2018. The latter year showed a drought response similar to Kaamanen: a higher annual CO_2 uptake was observed in the forest, while the mire ecosystem (9 % of the area) turned from an annual CO_2 sink to a source. The annual CO_2 balances of Svartberget

were comparable to Kaamanen, whose pine forest had an annual CO_2 balance of -78 and -119 g C m^{-2} during the first and second study year (Fig. 8d). In a synthesis by Virkkala et al. (2021), the mean annual NEE of 41 boreal biomes was on average -46 g C m^{-2} (uplands -47 g C m^{-2} and wetlands -38 g C m^{-2}); i.e. the CO_2 sink was lower in uplands and larger in wetlands than the mean landscape-scale sink in Kaamanen. These results show that there can be large spatial variation in C exchange among boreal ecosystems e.g. forests, but also part of the variation between landscape C balances derive from the ecosystem composition. ~~These results show that there is large spatial and temporal variation in C exchange among boreal landscapes, but a major part of this derives from the ecosystem composition.~~

The temporal variation of the landscape-level CO_2 flux (Fig. 13) obviously depended on the flux variation of individual ecosystems~~.~~, and different ecosystems showed different environmental responses. During the two study years there were three periods when the ecosystem-specific fluxes clearly deviated from each other, which differences were reflected in the landscape-level C balance. ~~However, different ecosystems showed different environmental responses, and during the two study years there were four periods the ecosystem-specific fluxes deviated from each other and that were reflected in the landscape-level C balance.~~ First, the warmer-than-average early growing season in 2018 increased the CO_2 uptake of the fen ecosystem (Fig. 9a) and probably also the pine bog fluxes (Figs. 11a, 12a), or conversely the colder-than-average early growing season 2017 led to lower CO_2 uptake by these ecosystems. However, equally large variation in the early growing season CO_2 uptake was not observed in the pine forest fluxes as the evergreen pine forest phenology differs from that of the largely deciduous mire ~~phenology~~. Second, the rainy peak growing season in 2017 increased the ER rates of the pine forest ecosystem compared to the same period the next year, which was much warmer, and thus the ER fluxes were similar (Figs. 8, A1). Conversely, at the fen the warm summer of 2018 increased the ER sum compared to the cool, rainy summer in 2017. This was due to the inherently different water balance between uplands and peatlands. ~~Second, the rainy peak growing season 2017 increased the ER of pine forest ecosystem compared to the same period the next year, which decreased the net CO_2~~CO_2~~ uptake (Figs. 8, A1). This was also reflected in the estimated pine bog fluxes (Figs. 11, 12), but not observed at the fen due to the inherently different water balance between uplands and peatlands.~~ Third, the drought period in summer 2018 decreased CO_2 uptake in both the pine forest and fen ecosystems (Figs. 8b, 9b), and the pine bogs likely showed a similar response.

The lakes in the landscape acted as CO_2 sources to the atmosphere throughout the growing seasons, with peak emissions linked with the spring thaw. However, the temporal variation in the lake emissions had only a minor effect on the temporal variation in the landscape-scale CO_2 fluxes as the flux magnitude did not vary as much on the lakes as on the terrestrial ecosystems during the growing seasons (Figs. 8, 9, 10). Integrated over the study area, the total lake emissions had a considerable effect on the landscape-scale annual balances (Fig. 14). ~~Finally, the cold spell in autumn 2018 reduced ER causing the forest to revert to a CO_2 sink (Fig. 8), but a similar effect was not observed for the fen. However, the effect of the cold spell was sufficiently strong to be discernible in the modelled pine bog ER fluxes (Figs. 11, 12).~~

As the pine forest and pine bog CH_4 fluxes used for upscaling were adopted from literature (Dinsmore et al., 2017; Bubier et al., 2005), only the fen and lake ecosystem CH_4 fluxes affect the annual variation in the upscaled landscape-level fluxes

850 (Figs. 13, 14). The CH$_4$ emissions from the fen decreased due to the drought in 2018 (Fig. 9e), thus decreasing the annual emissions compared to the first study year (Table A6~~5~~). However, as the modelled lake CH$_4$ emissions were slightly higher during the second year (Table 6), there was only a minor difference in the annual landscape-level CH$_4$ balance (Fig. 13f, Table A6).

During the two study years, the meteorological conditions were not optimal for C sequestration as the fen on average acted as
855 a weaker CO$_2$ sink than in some previous years (Aurela et al., 2007), and even a source in the second year. ~~However, as the emissions from lakes increased due to a longer ice-free period in the second year (Table 6), there was only a minor difference in the annual landscape-level CH$_4$ balance (Fig. 13f, Table A5).~~

~~During the two study years, the meteorological conditions were not optimal for C sequestration, as indicated by the lower fen ecosystem CO$_2$ sink than in some previous years (Aurela et al., 2007).~~ Thus, the landscape-level CO$_2$ uptake would probably
860 be higher in more optimal conditions. However, the conditions favouring C sequestration differ between ecosystems, as all terrestrial ecosystems are likely to sequester more CO$_2$ during longer growing seasons, but mires can simultaneously emit more CH$_4$, and lakes emit more both CO$_2$ and CH$_4$.

For estimating the relative radiative impact of the CO$_2$ and CH$_4$ exchanges in Kaamanen, the CH$_4$ flux was translated to CO$_2$-equivalent flux by multiplying it by the Sustained Global Warming Potential (SGWP) coefficient (Neubauer and Megonigal,
865 2015; Neubauer, 2021). If the CO$_2$ and CH$_4$ flux observed during the two study years continued for the next 500 yr (SGWP = 14 g CO$_2$-eq./g CH$_4$), the net CO$_2$-equivalent flux of the fen would be positive. However, in longer time scales the fen will eventually have a negative radiative balance even with a low annual CO$_2$ uptake. In addition to the time-dependent contribution of fens, the annual net CO$_2$-equivalent flux of the landscape was affected by uptake of both CO$_2$ and CH$_4$ by forests, i.e. a systematically negative CO$_2$-equivalent flux, and emissions of both CO$_2$ and CH$_4$ from lakes, i.e. a systematically positive
870 CO$_2$-equivalent flux. Assuming the present-day fluxes for each ecosystem, upscaling suggests that the net CO$_2$-equivalent flux of the landscape would be initially positive but turn negative soon after 100 yr (SGWP = 45 g CO$_2$-eq./g CH$_4$ for the 100 yr time horizon).
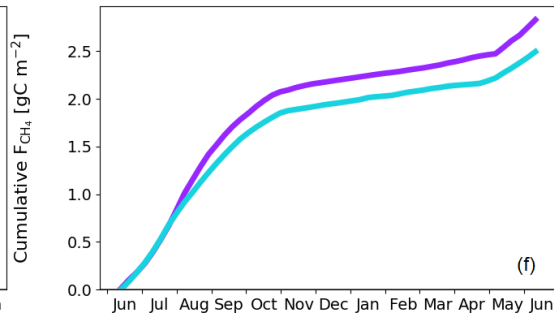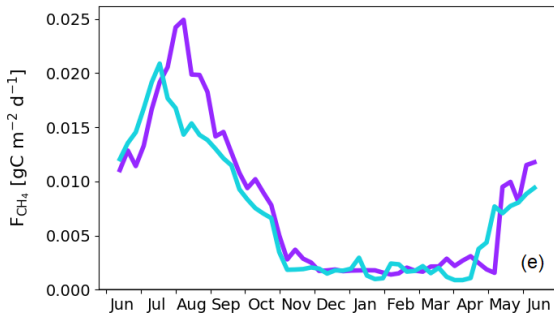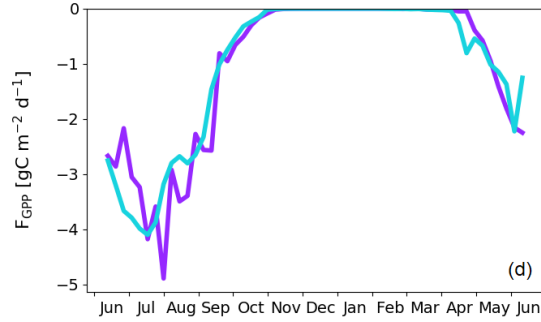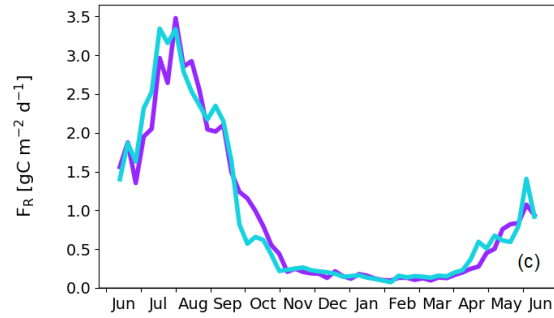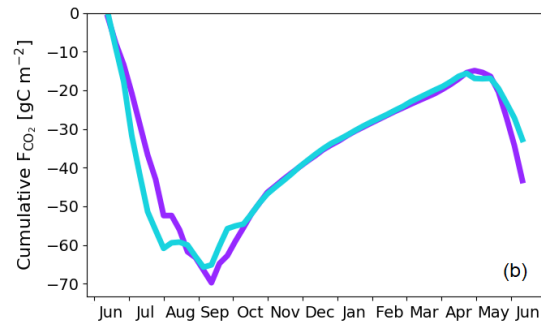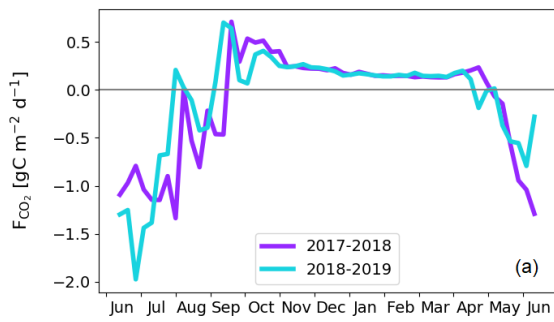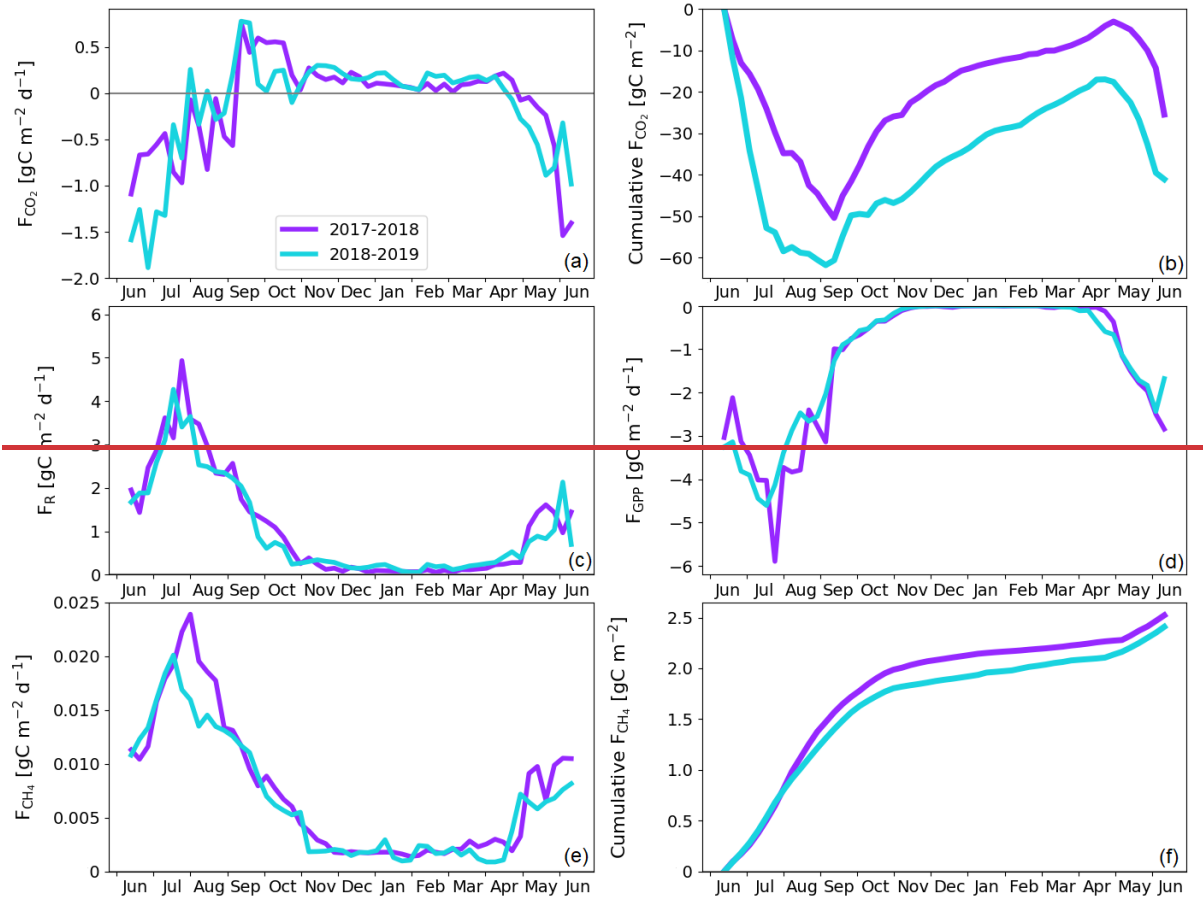
Figure 13. Landscape-level gap-filled fluxes. Weekly averaged CO_2 (a), ER (c), GPP (d) and CH_4 (e) flux, and cumulative CO_2 (b) and CH_4 (f) flux.
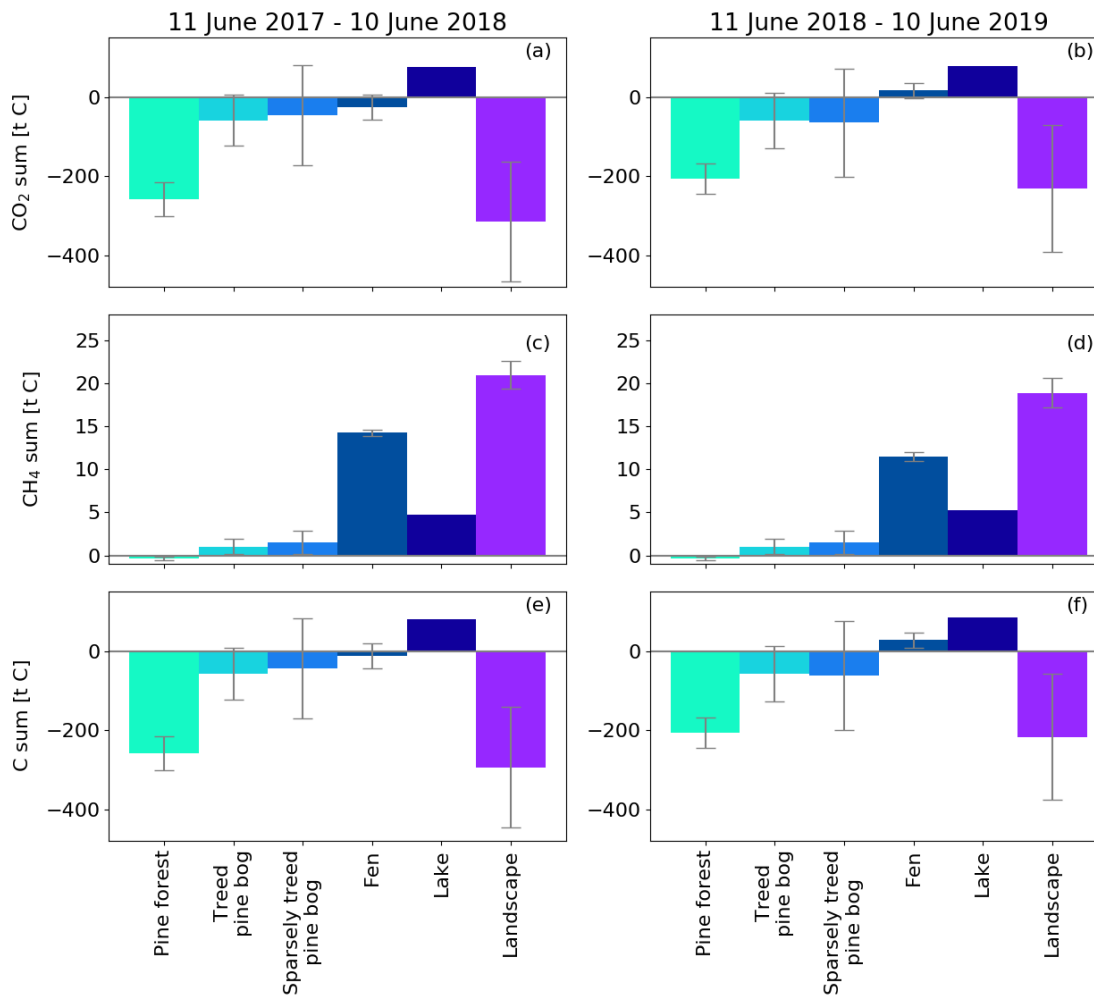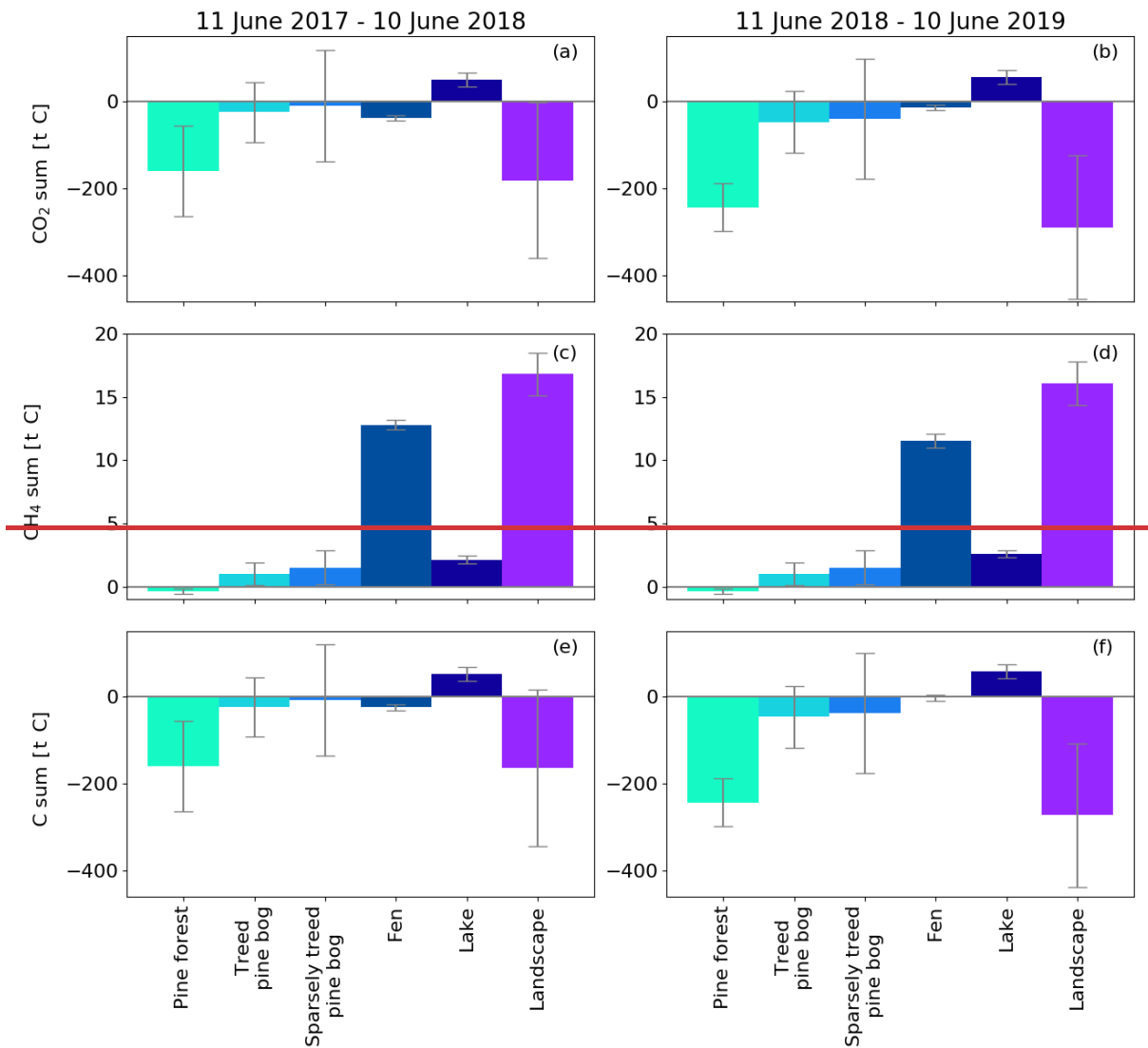
Figure 14. Annual CO_2, CH_4 and C flux sums for different ecosystems and the landscape (Fig. 1) upscaled with the corresponding area. The CH_4 flux estimate for forest is from Dinsmore et al. (2017) and for pine bog from Bubier et al. (2005). The error bars denote the 95 % confidence interval. Uncertainty estimates were not available for the modelled lake balances (Kou et al., 2022).

4 Conclusions

We estimated the ecosystem-atmosphere exchange of CO_2 and CH_4 for the main ecosystems in a subarctic landscape during two full years. The 7 km² study area consisted of pine forest, open peatlandpatterned flark fen, two pine bog ecosystems and two lake types. For the terrestrial ecosystems, C exchange was most sensitive to changes in temperature and moisture conditions, while on the lake it depended on the amount of available carbon in sediment and the length of the ice-free period.

The lakes in the study area released back to the atmosphere 24 % of the C that was sequestered by the landscape during the two-year study period, and there was a fourfold difference in the CO_2 emissions between organic- and mineral-sediment lakes. The lakes in the study area released 20 % of the C that was sequestered by the landscape during the study period, and there was a sixfold difference in the CO_2 emissions between organic- and mineral-sediment lakes. Thus, more measurements are needed to determine accurately define the role of lake emission variability. Similarly, the CH_4 fluxes were much greater from the organic--sediment lake, but the overall impact of lake fluxes on the landscape-scale was smaller than for CO_2. Obviously, the great difference in the observed C fluxes between the lake types should be considered when estimating regional-scale fluxes in a heterogeneous environment such as a northern boreal landscape.

There were three periods when the C fluxes of the terrestrial ecosystems were clearly different between the two study years due to meteorological conditions. In the pine forest, the CO_2 fluxes were affected by the rainy weather in summer 2017 increasing the ER rate to the level observed during the warmer growing season the following year. At the fen, however, the warm growing season in 2018 resulted in a higher ER sum than in the previous growing season, highlighting the differing water balance of the fen and upland forest ecosystems. The warmer-than-average early growing season in 2018 advanced the plant growth at the fen, thus increasing the CO_2 uptake of this ecosystem. All terrestrial ecosystems were affected by a short but severe drought event in July 2018, which decreased the GPP rates and thus CO_2 uptake. However, both the onset of and recovery from drought effects occurred more rapidly at the fen than in the pine forest. Additionally, during the drought the CH_4 emissions from the fen decreased due to water level drawdown and possibly also due to decreased plant root carbon input. There were four periods when the C fluxes of the terrestrial ecosystems were clearly different between the two study years due to meteorological conditions. In the pine forest, the CO_2 fluxes were affected by the rainy weather in summer 2017, as the high ER rates decreased the CO_2 uptake. The warmer-than-average early growing season in 2018 advanced the plant growth at the fen thus increasing the ecosystem CO_2 uptake. All terrestrial ecosystems were affected by a short but severe drought event in July 2018, which decreased the GPP rates and thus CO_2 uptake. However, both the onset of drought effect and the recovery from drought occurred more rapidly at the fen than in the pine forest. Additionally, during the drought the CH_4 emissions from the fen decreased due to water level drawdown and possibly also due to decreased plant root carbon input. Later, a cold spell in autumn 2018 reduced ER rates in the pine forest ecosystem. The CO_2 flux responses to changing environmental conditions were reflected in the landscape-level CO_2 fluxes, even though only the short and severe drought event affected the CO_2 fluxes of all terrestrial ecosystems similarly. For this reason, none of the ecosystems alone controlled the changes in the landscape-level CO_2 exchange. In contrast to the CO_2 fluxes, it appears that the landscape-level CH_4 flux and its variation can almost entirely be estimated based on the fen data.

Both study years had periods of nonoptimal C sequestration conditions, but still the landscape remained as a CO_2 sink., which This indicates that the multitude of ecosystems contributes positively to the landscape resilience to C loss.

Appendix A: Ancillary environmental information, flux and statistical tests

Table A1. Ground layer biomass and leaf area index (mean ± standard deviation) and the number of field measurement points.

Ground layer	Biomass [g dry matter m^{-2}]				Leaf area index [m^{-2} m^{-2}]			n
Land cover class	Shrubs	Forbs and graminoids	Mosses and lichens	Total	Shrubs	Forbs and graminoids	Total	
Pine forest	144.1 ± 73.0	3.2 ± 7.8	398.1 ± 200.7	545.4 ± 189.5	0.39 ± 0.15	0.02 ± 0.04	0.41 ± 0.17	75
Pine bog	284.9 ± 225.6	38.2 ± 30.2	398.4 ± 172.9	721.6 ± 324.5	0.51 ± 0.22	0.22 ± 0.16	0.73 ± 0.25	36
Fen	149.4 ± 90.9	69.6 ± 36.9	146.7 ± 169.1	365.6 ± 231.2	0.21 ± 0.10	0.37 ± 0.19	0.59 ± 0.21	223
String top [a]	247.5 ± 147.4	39.5 ± 29.9	261.8 ± 263.7	548.8 ± 318.8	0.50 ± 0.20	0.21 ± 0.14	0.71 ± 0.19	49

[a] String top CO_2 fluxes were used for estimating ~~in pine bog flux estimation for~~ the ground layer flux of pine bogs~~part, as the two ground layers resemble one another~~.

Table A2. Pine forest basal area, stand density and diameter at breast height (DBH) (mean ± standard deviation) derived from field measurements.

Tree species	Basal area	No. of trees per ha	DBH [cm]
Scots pine	13.2 ± 6.4	545 ± 827	15 ± 6
Downy birch	0.3 ± 0.7	103 ± 243	7 ± 6

Table A3~~2~~. Average tree height (mean ± standard deviation) and the number of field measurement points.

Ecosystem	Average tree height [m]	n
Pine forest	7.7 ± 2.0	43
Pine bog	4.9 ± 2.0	17

Table A4~~3~~. Soil and peat properties (mean ± standard deviation) for pine forest, pine bog and fen ecosystems. Except the pine forest organic layer, pH was always measured at 30 cm depth. In pine bog and fen ecosystems, bulk density, C and N content and C:N ratio are the mean of 0–5 and 15–20 cm peat layers.

Ecosystem	pH	Bulk density [g cm^{-3}]	Soil C content [mg cm^{-3}]	Soil N content [mg cm^{-3}]	C:N ratio	No. of sample plots
Pine forest	6.0 ± 0.4					11
Organic layer	4.6 ± 0.2	0.136 ± 0.101	52.9 ± 44.9	1.2 ± 0.9	43.5 ± 8.4	
Eluvial layer		1.037 ± 0.265	20.6 ± 11.9	0.5 ± 0.3	45.7 ± 11.2	
Illuvial layer top		1.219 ± 0.110	16.5 ± 10.4	0.5 ± 0.4	36.4 ± 9.3	
Illuvial layer bottom		1.337 ± 0.145	5.0 ± 4.1	0.2 ± 0.2	43.8 ± 40.1	
50 cm below organic layer		1.511 ± 0.124	2.1 ± 3.3	0.1 ± 0.2	42.4 ± 30.6	
100 cm below organic layer		1.588 ± 0.100	1.1 ± 0.9	0.01 ± 0.02	256 ± 506	

45

Pine bog	5.0 ± 0.3	0.146 ± 0.246	43.8 ± 29.6	1.2 ± 1.1	44.0 ± 11.8	8
Fen						
String top	4.6 ± 0.4	0.095 ± 0.030	50.9 ± 15.9	1.5 ± 0.8	38.9 ± 10.5	20
String margin	5.7 ± 0.5	0.094 ± 0.046	44.7 ± 21.5	2.5 ± 1.9	24.3 ± 13.0	16
Trichophorum tussock	5.9 ± 0.2	0.133 ± 0.042	57.2 ± 11.3	3.4 ± 0.8	17.1 ± 1.8	18
Flark	5.8 ± 0.2	0.098 ± 0.017	44.2 ± 8.6	2.7 ± 0.6	16.5 ± 2.2	18

Table A54. Tree biomass and leaf area index derived from field and remote sensing measurements.

Ecosystem	Tree biomass [g dry matter m^{-2}]	Tree leaf area index [m^{-2} m^{-2}]
Pine forest	3165	1.97
Treed pine bog	1649	1.02
Sparsely treed pine bog	514	0.32

940

Table A6. Annual CO_2, CH_4 and C balances of the five ecosystems and landscape. Uncertainty estimates were not available for the lake balances (Kou et al., 2022) and thus they are not taken into account in the landscape-scale uncertainty estimates.

	11 June 2017 – 10 June 2018	11 June 2018 – 10 June 2019
CO_2 balance [g C m^{-2}]		
Pine forest	-126 ± 10	-101 ± 9
Treed pine bog	-92 ± 102	-92 ± 110
Sparsely treed pine bog	-48 ± 134	-68 ± 145
Fen	-14 ± 7	9 ± 5
Lakes	53	56
Landscape	-45 ± 59	-33 ± 63
CH_4 balance [g C m^{-2}]		
Pine forest	-0.2 ± <0.1 [a]	-0.2 ± <0.1 [a]
Pine bog	1.6 ± 1.4 [b]	1.6 ± 1.4 [b]
Fen	7.8 ± 0.2	6.3 ± 0.3
Lakes	3.3	3.7
Landscape	3.0 ± 0.7	2.7 ± 0.7
C balance [g C m^{-2}]		
Pine forest	-126 ± 10	-101 ± 9
Treed pine bog	-90 ± 102	-90 ± 110
Sparsely treed pine bog	-46 ± 134	-66 ± 145
Fen	-7 ± 7	15 ± 5

Lakes	56	60
Landscape	-42 ± 59	-31 ± 63

[a] Dinsmore et al. (2017).

[b] Bubier et al. (2005).

Table A5. Annual CO_2, CH_4 and C flux balances of the five ecosystems and landscape. The lake flux balances of the second year include scaled estimates using the previous year's measurements on the organic sediment lake. Statistically significant differences between 2017 and 2018 are indicated with an asterisk (Z test, **: $p < 0.05$, *: $p < 0.10$ and ¨: $p < 0.20$).

	11th June 2017 – 10th June 2018	11th June 2018 – 10th June 2019	Difference
CO_2 balance [g C m^{-2}]			
Pine forest	-78.3 ± 50.8	-118.9 ± 26.8	-40.6 ¨
Treed pine bog	-39.1 ± 107.6	-75.0 ± 111.2	-35.9
Sparsely treed pine bog	-9.8 ± 135.4	-42.1 ± 145.3	-32.3
Fen	-20.6 ± 3.6	-7.6 ± 3.7	13.0 **
Lakes	35.6 ± 11.2	(39.0 ± 11.3)	
Landscape	-25.9 ± 65.7	-41.3 ± 64.9	-15.4
CH_4 balance [g C m^{-2}]			
Pine forest	-0.2 ± <0.1 [a]	-0.2 ± <0.1 [a]	
Pine bog	1.6 ± 1.4 [b]	1.6 ± 1.4 [b]	
Fen	7.0 ± 0.2	6.3 ± 0.3	-0.7 **
Lakes	1.5 ± 0.2	(1.8 ± 0.2)	
Landscape	2.4 ± 0.7	2.3 ± 0.7	-0.1
C balance [g C-^{CH_4}m^{-2}]			
Pine forest	-78.5 ± 50.8	-119.1 ± 26.8	-40.6 ¨
Treed pine bog	-37.5 ± 107.6	-73.4 ± 111.2	-35.9
Sparsely treed pine bog	-8.2 ± 135.4	-40.5 ± 145.3	-32.3
Fen	-13.6 ± 3.6	-1.3 ± 3.7	12.3 **
Lakes	37.1 ± 11.2	(40.8 ± 11.3)	
Landscape	-23.5 ± 65.7	-39.0 ± 64.9	-15.5

[a] From Dinsmore et al. (2017).

[b] From Bubier et al. (2005). **Table A6:** Monthly ER, GPP, NEE and CH_4 flux sums. Statistically significant differences between 2017 and 2018 are indicated with an asterisk (Z test, **: $p < 0.05$, *: $p < 0.10$ and ¨: $p < 0.20$).

	ER [g C m^{-2}]			GPP [g C m^{-2}]			NEE [g C m^{-2}]			CH_4 ex
Pine forest	2017	2018	Change	2017	2018	Change	2017	2018	Change	2017
June (11-30)	72.8 ± 22.2	59.7 ± 15.4	-13.1	116.8 ± 29.0	117.7 ± 26.7	0.9	-44.4 ± 36.6	-57.5 ± 30.8	-13.1	
July	240.3 ± 70.9	186.4 ± 37.5	-53.9 ¨	253.3 ± 72.4	219.6 ± 48.4	-33.7	-11.8 ± 101.4	-32.4 ± 61.2	-20.6	
August	173.8 ± 37.5	138.0 ± 27.0	-35.8 ¨	182.6 ± 42.7	139.8 ± 37.9	-42.8 ¨	-9.0 ± 56.8	-1.2 ± 46.5	7.8	

47

	2017	2018	Change	2017	2018	Change	2017	2018	Change	2017
September	106.5±58.3	88.0±17.5	-18.5	96.7±79.5	79.4±40.5	-17.3	10.8±98.5	9.1±44.2	-1.6	
October	43.6±40.5	25.0±10.5	-18.6	31.7±36.5	31.6±7.3	-0.1	12.7±54.5	-7.8±12.7	-20.4	
Treed pine bog	2017	2018	Change	2017	2018	Change	2017	2018	Change	2017
June (11-30)	64.7±23.1	48.6±13.5	-16.0	86.8±21.8	96.6±21.1	9.8	-22.4±31.7	-47.7±25.0	-25.3	
July	185.5±65.7	151.1±43.8	-34.4	197.9±58.2	191.5±46.3	-6.5	-11.8±87.8	-40.0±63.7	-28.1	
August	131.6±28.8	112.5±31.8	-19.1	151.4±33.0	118.1±31.6	-33.4¨	-19.9±43.8	-5.3±44.9	14.7	
September	77.9±42.3	75.5±13.3	-2.4	71.5±57.4	59.9±29.5	-11.6	6.9±71.3	15.9±32.3	9.0	
October	34.4±29.2	20.9±7.6	-13.5	19.6±26.3	19.6±5.4	0.0	15.2±39.3	0.8±9.3	-14.4	
Sparsely treed pine bog	2017	2018	Change	2017	2018	Change	2017	2018	Change	2017
June (11-30)	58.6±23.5	40.4±11.7	-18.2¨	64.3±14.0	80.8±15.5	16.5¨	-5.9±27.3	-40.3±19.4	-34.5 **	
July	144.3±60.9	124.6±47.4	-19.7	156.4±44.4	170.3±44.2	13.9	-11.9±75.4	-45.6±64.8	-33.7	
August	99.9±19.7	93.4±34.7	-6.6	128.1±23.2	101.8±25.8	-26.3¨	-28.2±30.4	-8.3±43.2	19.8	
September	56.5±24.0	66.1±8.8	9.7	52.6±32.0	45.3±17.0	-7.4	4.0±40.0	20.9±19.2	17.0	
October	27.6±16.3	17.9±4.4	-9.6	10.6±14.6	10.6±3.3	0.0	17.1±21.9	7.2±5.5	-9.9	
Fen	2017	2018	Change	2017	2018	Change	2017	2018	Change	2017
June (11-30)	22.8±5.1	28.2±7.0	5.4	27.6±3.9	49.2±7.3	21.5 **	-4.8±6.4	-21.0±10.1	-16.2 **	0.56±0.02
July	68.2±14.9	71.5±14.2	3.3	119.3±14.8	107.2±18.2	-12.0	-51.0±21.1	-35.7±23.1	15.3	1.83±0.03
August	68.1±15.5	61.4±15.8	-6.7	86.8±16.3	71.4±12.3	-15.3¨	-18.7±22.5	-10.0±20.0	8.7	1.78±0.06
September	36.3±6.2	35.6±17.2	-0.7	25.6±8.3	20.8±12.5	-4.8	10.7±10.3	14.7±21.3	4.1	0.85±0.02
October	16.7±6.2	13.2±3.7	-3.5	4.7±17.2	2.8±6.8	-2.0	11.9±18.3	10.4±7.7	-1.5	0.46±0.01
Lake	2017	2018[a]	Change	2017	2018	Change	2017	2018[a]	Change	2017
June (11-30)	4.6±2.0	(5.3±2.1)					4.6±2.0	(5.3±2.1)		0.18±0.03
July	6.5±3.0	(5.8±2.3)					6.5±3.0	(5.8±2.3)		0.30±0.17
August	5.9±2.3	(5.8±2.6)					5.9±2.3	(5.8±2.6)		0.28±0.09
September	6.7±3.5	(6.8±2.8)					6.7±3.5	(6.8±2.8)		0.23±0.04
October	6.1±2.3	(6.1±2.3)					6.1±2.3	(6.1±2.3)		0.25±0.02
Landscape	2017	2018[a]	Change	2017	2018	Change	2017	2018[a]	Change	2017
June (11-30)	41.9±16.8	35.7±11.0	-6.2	57.9±18.1	66.9±17.4	9.0	-16.1±24.8	-30.9±20.6	-14.8	0.18±0.02
July	125.6±50.0	104.8±31.2	-20.8	144.2±47.2	132.5±35.6	-11.7	-18.1±68.8	-27.4±47.3	-9.3	0.54±0.08
August	95.2±24.9	80.4±23.5	-14.8	107.0±28.2	83.9±25.7	-23.1	-11.9±37.7	-3.4±34.8	8.5	0.52±0.05
September	56.6±35.8	52.2±14.2	-4.4	48.6±48.7	40.2±25.7	-8.4	8.5±60.5	12.2±29.3	3.7	0.27±0.02
October	25.2±24.9	16.3±6.8	-8.9	13.7±24.0	13.2±5.7	-0.5	11.7±34.6	2.7±8.9	-9.0	0.17±0.01

[a] Flux estimates of 2018 include organic lake flux measurements from 2017.

Table A7. Data sources for different ecosystems

Ecosystem	Eddy covariance measurements	Flux chamber measurements	Pine bog flux model (Sect 2.4)	Arctic Lake Biogeochemistry Model (Kou et al., 2022)	Estimate from literature
Pine forest	CO_2				CH_4 [a]
Fen	CO_2, CH_4	CO_2, CH_4			
Lakes		CO_2, CH_4		CO_2, CH_4	
Pine bog			CO_2		CH_4 [b]

[a] Dinsmore et al. (2017).

[b] Bubier et al. (2005).

955
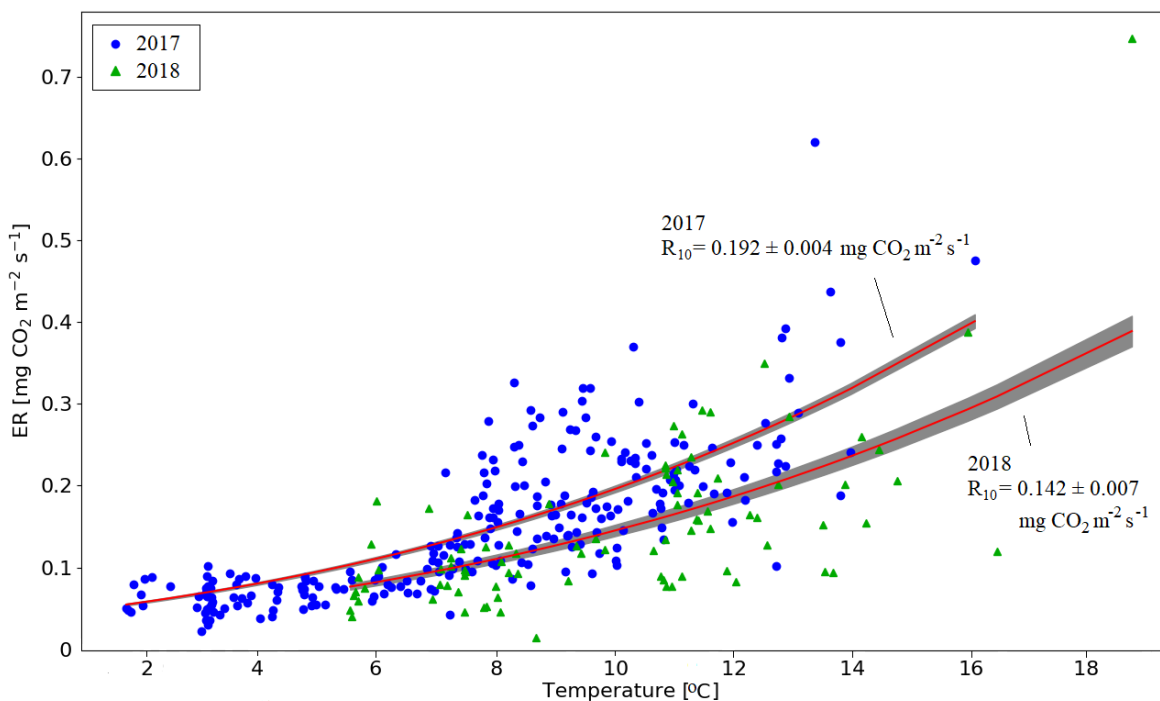
Figure A1. ~~Pine forest ER t~~Temperature response of ecosystem respiration in the pine forest ~~curves~~based on~~,~~ the ~~N~~nighttime EC data 15 June – 15 August 2017 and 2018. The lines show the fitted temperature response $ER = R_{10} \times e^{E_0\left(\frac{1}{56.02} - \frac{1}{T-227.13}\right)}$, with $E_0 = 400$ K^{-1} (Lloyd and Taylor, 1994). The shaded areas indicate the one-~~-~~sigma confidence intervals.
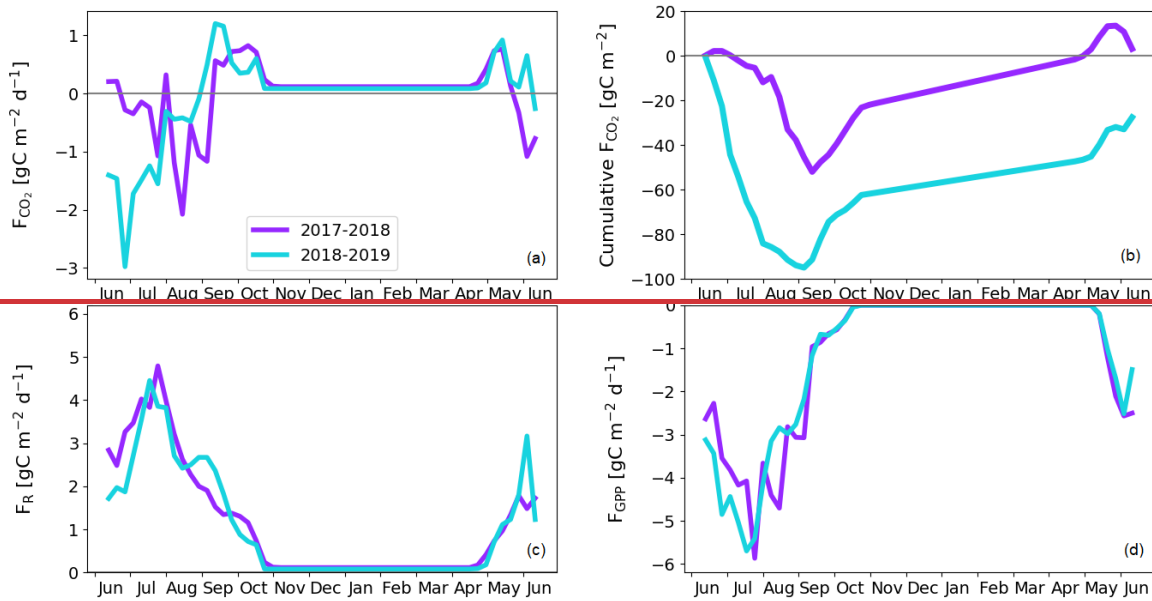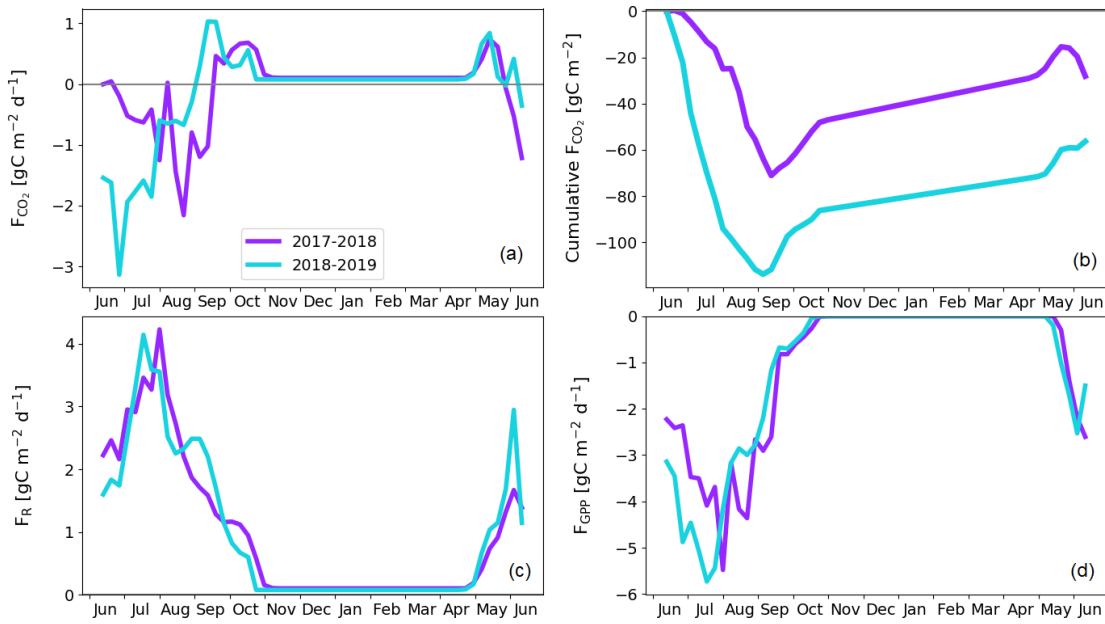
Figure A2. String top gap-filled fluxes. Weekly averaged (a) and cumulative CO_2 flux (b), and weekly averaged ER (c) and GPP (d) flux, used for estimating pine bog ecosystem fluxes.

Table A87. Average bulk density, C and N content and C:N ratio (± standard deviation) in the top 20 cm of lake sediments.

Lake	Bulk density [g cm^{-3}]	Soil C content of dry mass [%]	Soil N content of dry mass [%]	C:N ratio	No. of core samples
Jänkäjärvi (organic sediment lake)	0.13 ± 0.03	30.3 ± 1.6	1.6 ± 0.1	18.4 ± 1.0	1
Jänkälampi (mineral sediment lake)					
Northern basin	0.91 ± 0.47	5.5 ± 5.4	0.3 ± 0.3	19.9 ± 6.2	4
Southern basin	0.13 ± 0.10	22.6 ± 3.1	1.4 ± 0.4	15.6 ± 2.7	1

References

990 Aguadé, D., Poyatos, R., Gómez, M., Oliva, J. and Martínez-Vilalta, J.: The role of defoliation and root rot pathogen infection in driving the mode of drought-related physiological decline in Scots pine (Pinus sylvestris L.), Tree Physiol., 35, 229-242, doi:10.1093/treephys/tpv005, 2015.

Alm, J., Schulman, L., Walden, J., Nykänen, H., Martikainen, P. J., and Silvola, J.: Carbon Balance of a Boreal Bog during a Year with an Exceptionally Dry Summer, Ecology, 80, 161–174, https://doi.org/10.1890/0012-995 9658(1999)080[0161:CBOABB]2.0.CO;2, 1999.

Aubinet, M., Vesala, T., and Papale, D.: Eddy Covariance: A Practical Guide to Measurement and Data Analysis, Springer Netherlands, Dordrecht, https://doi.org/10.1007/978-94-007-2351-1, 2012.

Aurela, M., Laurila, T., and Tuovinen, J.-P: Seasonal CO_2 balances of a subarctic mire, J. Geophys. Res.-Atmos., 106, 1623–1637, https://doi.org/10.1029/2000JD900481, 2001.

1000 Aurela, M., Laurila, T., and Tuovinen, J.-P.: Annual CO₂CO2 balance of a subarctic fen in northern Europe: Importance of the wintertime efflux, J. Geophys. Res.-Atmos., 107, 4607, https://doi.org/10.1029/2002JD002055, 2002.

Aurela, M., Laurila, T., and Tuovinen, J.-P.: The timing of snow melt controls the annual CO_2 balance in a subarctic fen, Geophys. Res. Lett., 31, L16119, https://doi.org/10.1029/2004GL020315, 2004.

Aurela, M., Riutta, T., Laurila, T., Tuovinen, J.-P., Vesala, T., Tuittila, E., Rinne, J., Haapanala, S., and Laine, J.: CO_2 exchange 1005 of a sedge fen in southern Finland-the impact of a drought period, Tellus B, 59, 826–837, https://doi.org/10.1111/j.1600-0889.2007.00309.x, 2007.

Aurela M., Lohila A., Tuovinen J.-P., Hatakka J., Penttilä T. and Laurila T.: Carbon dioxide and energy flux measurements in four northern-boreal ecosystems at Pallas. Boreal Env. Res. 20: 455–473, 2015.

Barton, K.: MuMIn: Multi-Model Inference. R package version 1.43.17. https://CRAN.R-project.org/package=MuMIn (last 1010 access 1 October 2021), 2020.

Bastviken, D., Cole, J., Pace, M. and Tranvik, L.: Methane emissions from lakes: Dependence of lake characteristics, two regional assessments, and a global estimate, Global Biogeochem. Cycles, 18, GB4009, doi:10.1029/2004GB002238, 2004.

Bond-Lamberty, B., Peckham, S. D., Ahl, D. E., and Gower, S. T.: Fire as the dominant driver of central Canadian boreal forest carbon balance. Nature, 450, 89–92. https://doi.org/10.1038/nature06272, 2007.

1015 Breiman, L.: Random forests. *Machine learning*, *45*(1), 5-32, 2001.

Bubier, J. L., Crill, P. M., Moore, T. R., Savage, K., and Varner, R. K.: Seasonal patterns and controls on net ecosystem CO_2 exchange in a boreal peatland complex, Global Biogeochem. Cy., 12, 703–714, https://doi.org/10.1029/98GB02426, 1998.

Bubier, J., Moore, T., Savage, K. and Crill, P.: A comparison of methane flux in a boreal landscape between a dry and a wet year, Global Biogeochem. Cycles, 19, GB1023-n/a, doi:10.1029/2004GB002351, 2005.

1020 Büker, P., Morrissey, T., Briolat, A., Falk, R., Simpson, D., Tuovinen, J.-P., Alonso, R., Barth, S., Baumgarten, M., Grulke, N., Karlsson, P. E., King, J., Lagergren, F., Matyssek, R., Nunn, A., Ogaya, R., Penuelas, J., Rhea, L., Schaub, M., Uddling, J., Werner, W. and Emberson, L. D.: DO3SE modelling of soil moisture to determine ozone flux to forest trees, Atmospheric chemistry and physics, 12, 5537-5562, doi:10.5194/acp-12-5537-2012, 2012.

Chapin, F. S., Matson, P. A., and Vitousek, P.: Principles of Terrestrial Ecosystem Ecology (Second Edition), Springer, 1025 https://doi.org/10.1007/978-1-4419-9504-9, 2011.

Chen, T, and Guestrin, C. Xgboost: A scalable tree boosting system. Proceedings of the 22nd acm sigkdd international conference on knowledge discovery and data mining, 785-794, 2016.

Chi, J., Nilsson, M. B., Laudon, H., Lindroth, A., Wallerman, J., Fransson, J. E. S., Kljun, N., Lundmark, T., Ottosson Löfvenius, M. and Peichl, M.: The Net Landscape Carbon Balance—Integrating terrestrial and aquatic carbon fluxes in a 1030 managed boreal forest landscape in Sweden, Global Change Biol., 26, 2353-2367, doi:10.1111/gcb.14983, 2020.

Cole, J. J., Prairie, Y. T., Caraco, N. F., McDowell, W. H., Tranvik, L. J., Striegl, R. G., Duarte, C. M., Kortelainen, P., Downing, J. A., Middelburg, J. J., and Melack, J.: Plumbing the global carbon cycle: Integrating inland waters into the terrestrial carbon budget. Ecosystems, 10(1), 171-184. https://doi.org/10.1007/s10021-006-9013-8, 2007.

Denfeld, B. A., Lupon, A., Sponseller, R. A., Laudon, H. and Karlsson, J.: Heterogeneous CO_2 and CH_4 patterns across space 1035 and time in a small boreal lake, Inland Waters, 10:3, 348-359, DOI: 10.1080/20442041.2020.1787765, 2020.

Deppe, M., Knorr, K-H., McKnight, D. M., and Blodau, C.: Effects of short-term drying and irrigation on CO_2 and CH_4 production and emission from mesocosms of a northern bog and an alpine fen, Biogeochemistry, 100, 89–103, https://doi.org/10.1007/s10533-010-9406-9, 2010.

Dinsmore, K. J., Drewer, J., Levy, P. E., George, C., Lohila, A., Aurela, M. and Skiba, U. M.: Growing season CH_4 and N_2O 1040 fluxes from a subarctic landscape in northern Finland; from chamber to landscape scale. Biogeosciences, 14(4), 799–815. https://doi.org/10.5194/bg-14-799-2017, 2017.

Du, Y., Wang, Y., Su, F., Jiang, J., Wang, C., Yu, M. and Yan, J.: The response of soil respiration to precipitation change is asymmetric and differs between grasslands and forests, Global Change Biol., 26, 6015-6024, doi:10.1111/gcb.15270, 2020.

Foken, T. and Wichura, B.: Tools for quality assessment of surface-based flux measurements, Agr. Forest Meteorol., 78, 83– 1045 105, https://doi.org/10.1016/0168-1923(95)02248-1, 1996.

Fronzek, S., Carter, T., Räisänen, J., Ruokolainen, L., Luoto, M.: Applying probabilistic projections of climate change with impact models: A case study for sub-arctic palsa mires in Fennoscandia. Climatic Change. 99. 515-534. https://doi.org/10.1007/s10584-009-9679-y, 2010.

Gao, Y., Markkanen, T., Aurela, M., Mammarella, I., Thum, T., Tsuruta, A., Yang, H. and Aalto, T.: Response of water use efficiency to summer drought in a boreal Scots pine forest in Finland, Biogeosciences, 14, 4409–4422, https://doi.org/10.5194/bg-14-4409-2017, 2017.

Guo, M., Zhuang, Q., Tan, Z., Shurpali, N., Juutinen, S., Kortelainen, P., Martikainen, P. J.: Rising methane emissions from boreal lakes due to increasing ice-free days, Environ. Res. Lett., 15, 064008, https://doi.org/10.1088/1748-9326/ab8254, 2020.

Hadden, D. and Grelle, A.: Net CO_2 emissions from a primary boreo-nemoral forest over a 10 year period. Forest Ecology and Management, 398, 164–173. https://doi.org/10.1016/j.foreco.2017.05.008, 2017.

Hargreaves, K. J., Fowler, D., Pitcairn, C. E. R., and Aurela, M.: Annual methane emission from Finnish mires estimated from eddy covariance campaign measurements, Theor. Appl. Climatol., 70, 203–213, https://doi.org/10.1007/s007040170015, 2001.

Heiskanen, L., Tuovinen, J.-P., Räsänen, A., Virtanen, T., Juutinen, S., Lohila, A., Penttilä, T., Linkosalmi, M., Mikola, J., Laurila, T., and Aurela, M.: Carbon dioxide and methane exchange of a patterned subarctic fen during two contrasting growing seasons, Biogeosciences, 18, 873–896, https://doi.org/10.5194/bg-18-873-2021, 2021.

Heiskanen, L., Tuovinen, J-P., Vekuri, H., Räsänen, A., Virtanen, T., Juutinen, S., Vekuri, H., Lohila, A., Mikola, J., and Aurela, M.: Meteorological responses of carbon dioxide and methane fluxes in the terrestrial and aquatic ecosystems of a subarctic landscape [Data set], Zenodo, https://doi.org/10.5281/zenodo.7437333, (Version v2) https://doi.org/10.5281/zenodo.6334237, 2022.

Irvin, J., Zhou, S., McNicol, G., Lu, F., Liu, V., Fluet-Chouinard, E., ... and Jackson, R. B. Gap-filling eddy covariance methane fluxes: Comparison of machine learning model predictions and uncertainties at FLUXNET-CH4 wetlands. *Agricultural and Forest Meteorology*, *308*, 108528. 2021.

Jammet, M., Dengel, S., Kettner, E., Parmentier, F.-J. W., Wik, M., Crill, P., and Friborg, T.: Year-round CH_4 and CO_2 flux dynamics in two contrasting freshwater ecosystems of the subarctic, Biogeosciences, 14, 5189–5216, https://doi.org/10.5194/bg-14-5189-2017, 2017.

Jansen, J., Thornton, B. F., Cortés, A., Snöälv, J., Wik, M., MacIntyre, S., and Crill, P. M.: Drivers of diffusive CH_4 emissions from shallow subarctic lakes on daily to multi-year timescales, Biogeosciences, 17, 1911–1932, https://doi.org/10.5194/bg-17-1911-2020, 2020.

Jones, H. G.: Plants and Microclimate: A Quantitative Approach to Environmental Plant Physiology, Cambridge University Press, West Nyack, https://doi.org/10.1017/CBO9780511845727, 2013.

Juutinen, S., Väliranta, M., Kuutti, V., Laine, A. M., Virtanen, T., Seppä, H., Weckström, J. and Tuittila, E-S.: Short-term and long-term carbon dynamics in a northern peatland-stream-lake continuum: A catchment approach, J.Geophys.Res.Biogeosci., 118, 171-183, doi:10.1002/jgrg.20028, 2013.

1080   Kätterer, T., Reichstein, M., Andrén, O., and Lomander, A.: Temperature dependence of organic matter decomposition: a critical review using literature data analyzed with different models. Biol. Fertil. Soils 27, 258–262, https://doi.org/10.1007/s003740050430, 1998.

Kljun, N., Black, T. A., Griffis, T. J., Barr, A. G., Gaumont-Guay, D., Morgenstern, K., McCaughey, J. H. and Nesic, Z.: Response of net ecosystem productivity of three boreal forest stands to drought. Ecosystems, 10, 1039–1055.
1085   https://doi.org/10.1007/s10021-007-9088-x, 2007.

Kou, D., Virtanen, T., Treat, C. C., Tuovinen, J.-P., Räsänen, A., Juutinen, S., et al. Peatland heterogeneity impacts on regional carbon flux and its radiative effect within a boreal landscape. Journal of Geophysical Research: Biogeosciences, 127, e2021JG006774. https://doi.org/10.1029/2021JG006774, 2022.

Kulmala, L., Pumpanen, J., Kolari, P., Dengel, S., Berninger, F., Köster, K., ... and Bäck, J. Inter-and intra-annual dynamics
1090   of photosynthesis differ between forest floor vegetation and tree canopy in a subarctic Scots pine stand. *Agricultural and Forest Meteorology*, *271*, 1-11, 2019.

Laurila, T., Soegaard, H., Lloyd, C. R., Aurela, M., Tuovinen, J.-P., and Nordstroem, C.: Seasonal variations of net CO_2 exchange in European Arctic ecosystems, Theor. Appl. Climatol., 70, 183– 201, https://doi.org/10.1007/s007040170014, 2001.

Laurila T., Tuovinen J.-P., Lohila A., Hatakka J., Aurela M., Thum T., Pihlatie M., Rinne J. and Vesala T.: Measuring methane
1095   emissions from a landfill using a cost effective micrometeorological method. Geophys. Res. Let. 32: LI9808, https://doi.org/10.1029/2005GLO23462, 2005.

Lehtonen, I. and Pirinen, P.: 2018: An exceptionally warm thermal growing season in Finland, in: FMI's Climate Bulletin: Research Letters, Helsinki, Finnish Meteorological Institute, https://doi.org/10.35614/ISSN-2341-6408-IK-2019-03-RL, 2019a.

1100   Lehtonen, I. and Pirinen, P.: 2018: An exceptionally dry thermal growing season in Finland, in: FMI's Climate Bulletin: Research Letters, Helsinki, Finnish Meteorological Institute, https://doi.org/10.35614/ISSN-2341-6408-IK-2019-04-RL, 2019b.

Le Mer, J. and Roger, P.: Production, oxidation, emission and consumption of methane by soils: A review, European Journal of Soil Biology, 37(1), 25–50, https://doi.org/10.1016/S1164-5563(01)01067-6, 2001.

1105   Liaw, A., and Wiener, M.: Classification and regression by randomForest. *R news*, *2*(3), 18-22, 2002.

Lindroth, A., Lund, M., Nilsson, M., Aurela, M., Christensen, T. R., Laurila, T., Rinne, J., Riutta, T., Sagerfors, J., StröM, L., Tuovinen, J. and Vesala, T.: Environmental controls on the CO_2 exchange in north European mires, 59, 812-825, doi:10.1111/j.1600-0889.2007.00310.x, 2007.

Lindroth, A., Lagergren, F., Aurela, M., Bjarnadottir, B., Christensen, T., Dellwik, E., Grelle, A., Ibrom, A., Johansson, T.,
1110   Lankreijer, H., Launiainen, S., Laurila, T., Mölder, M., Nikinmaa, E., Pilegaard, K., Sigurdsson, B. D., and Vesala, T.: Leaf area index is the principal scaling parameter for both gross photosynthesis and ecosystem respiration of Northern deciduous

and coniferous forests. Tellus. Series B, Chemical and Physical Meteorology, 60(2). https://doi.org/10.3402/tellusb.v60i2.16909, 2008.

Lindroth, A., Holst, J., Linderson, M., Aurela, M., Biermann, T., Heliasz, M., Chi, J., Ibrom, A., Kolari, P., Klemedtsson, L., Krasnova, A., Laurila, T., Lehner, I., Lohila, A., Mammarella, I., Mölder, M., Löfvenius, M. O., Peichl, M., Pilegaard, K., Soosar, K., Vesala, T., Vestin, P., Weslien, P. and Nilsson, M.: Effects of drought and meteorological forcing on carbon and water fluxes in Nordic forests during the dry summer of 2018, Philos. Trans. R. Soc. Lond. , B, Biol. Sci., 375, 20190516, doi:10.1098/rstb.2019.0516, 2020.

Linkosalmi, M., Tuovinen, J.-P., Nevalainen, O., Peltoniemi, M., Taniş, C. M., Arslan, A. N., Rainne, J., Lohila, A., Laurila, T., and Aurela, M.: Tracking vegetation phenology of pristine northern boreal peatlands by combining digital photography with CO_2 flux and remote sensing data, Biogeosciences, 19, 4747–4765, https://doi.org/10.5194/bg-19-4747-2022, 2022.

Lloyd, J. and Taylor, J. A.: On the Temperature Dependence of Soil Respiration, Funct. Ecol., 8, 315–323, https://doi.org/10.2307/2389824, 1994.

Lohila, A., Tuovinen, J.-P., Hatakka, J., Aurela, M., Vuorenmaa, J., Haakana, M. and Laurila, T.: Carbon dioxide and energy fluxes over a northern boreal lake, Boreal Environ. Res., 20, 474-488, ISSN 1797-2469 (online), 2015.

Maanavilja, L., Riutta, T., Aurela, M., Laurila, T., and Tuittila, E-S.: Spatial variation in CO_2 exchange at a northern aapa mire, Biogeochemistry, 104, 325–345, https://doi.org/10.1007/s10533-010-9505-7, 2011.

Martín-Gómez, P., Aguilera, M., Pemán, J., Gil-Pelegrín, E., and Ferrio, J. P.: Contrasting ecophysiological strategies related to drought: the case of a mixed stand of Scots pine (*Pinus sylvestris*) and a submediterranean oak (*Quercus subpyrenaica*), Tree Physiology, Vol. 37, 11, 1478–1492, https://doi.org/10.1093/treephys/tpx101, 2017.

Masson-Delmotte, V., Zhai, P., Pörtner, H.-O., Roberts, D., Skea, J., Shukla, P. R., Pirani, A., Moufouma-Okia, W., Péan, C., Pidcock, R., Connors, S., Matthews, J. B. R., Chen, Y., Zhou, X., Gomis, M. I., Lonnoy, E., Maycock, T., Tignor, M., and Waterfield T.: Global Warming of 1.5°C. An IPCC Special Report on the impacts of global warming of 1.5°C above pre-industrial levels and related global greenhouse gas emission pathways, in the context of strengthening the global response to the threat of climate change, sustainable development, and efforts to eradicate poverty, World Meteorological Organization, Geneva, Switzerland, 2018.

Matkala, L., Kulmala, L., Kolari, P., Aurela, M., and Bäck, J.: Resilience of subarctic Scots pine and Norway spruce forests to extreme weather events. Agricultural and Forest Meteorology, 296. https://doi.org/10.1016/j.agrformet.2020.108239, 2021.

McElligott, K. M., Seiler, J. R. and Strahm, B. D.: The Impact of Water Content on Sources of Heterotrophic Soil Respiration, Forests, 8, 299, doi:10.3390/f8080299, 2017.

McMillen, R. T.: An eddy correlation technique with extended applicability to non-simple terrain, Bound.-Lay. Meteorol., 43, 231–245, https://doi.org/10.1007/BF00128405, 1988.

Mekonnen, Z. A., Riley, W. J., Berner, L. T., Bouskill, N. J., Torn, M. S., Iwahana, G., Breen, A. L., Myers-Smith, I. H., García Criado, M., Liu, Y., Euskirchen, E. S., Goetz, S. J., Mack, M. C. and Grant, R. F.: Arctic tundra shrubification: a

1145 review of mechanisms and impacts on ecosystem carbon balance, Environ. Res. Lett. 16, 053001, https://doi.org/10.1088/1748-9326/abf28b, 2021.

Meyer, N., Welp, G., and Amelung, W.: The temperature sensitivity (Q10) of soil respiration: controlling factors and spatial prediction at regional scale based on environmental soil classes. Global Biogeochem. Cycles 32, 306–323, https://doi.org/10.1002/2017GB005644, 2018.

1150 Montagnani, L., Grünwald, T., Kowalski, A., Mammarella, I., Merbold, L., Metzger, S., Sedlák, P. and Siebicke, L.: Estimating the storage term in eddy covariance measurements: the ICOS methodology, International Agrophysics, 32, 551-567, doi:10.1515/intag-2017-0037, 2018.

Moyano, F. E., Vasilyeva, N., Bouckaert, L., Cook, F., Craine, J., Curiel Yuste, J., Don, A., Epron, D., Formanek, P., Franzluebbers, A., Ilstedt, U., Kätterer, T., Orchard, V., Reichstein, M., Rey, A., Ruamps, L., Subke, J. -., Thomsen, I. K. and
1155 Chenu, C.: The moisture response of soil heterotrophic respiration: interaction with soil properties, Biogeosciences, 9, 1173-1182, doi:10.5194/bg-9-1173-2012, 2012.

Muilu-Mäkelä, R., Vuosku, J., Läärä, E., Saarinen, M., Heiskanen, J., Häggman, H. and Sarjala, T.: Water availability influences morphology, mycorrhizal associations, PSII efficiency and polyamine metabolism at early growth phase of Scots pine seedlings, Plant Physiol. Biochem., 88, 70-81, doi:10.1016/j.plaphy.2015.01.009, 2015.

1160 Neubauer, S.C. and Megonigal, J.P.: Moving Beyond Global Warming Potentials to Quantify the Climatic Role of Ecosystems, Ecosystems 18, 1000–1013, https://doi.org/10.1007/s10021-015-9879-4, 2015.

Neubauer, S.C.: Global Warming Potential Is Not an Ecosystem Property, Ecosystems 24, 2079–2089, https://doi.org/10.1007/s10021-021-00631-x, 2021.

Orchard, V. A. and Cook, F. J.: Relationship between soil respiration and soil moisture, Soil Biol. Biochem., Vol. 15, No. 4,
1165 pp. 447-453, 1983.

Papale, D., Reichstein, M., Aubinet, M., Canfora, E., Bernhofer, C., Kutsch, W., ... and Yakir, D. Towards a standardized processing of Net Ecosystem Exchange measured with eddy covariance technique: algorithms and uncertainty estimation. *Biogeosciences, 3*(4), 571-583. 2006.

Piilo, S. R., Korhola, A., Heiskanen, L., Tuovinen, J-P., Aurela, M., Juutinen, S., Marttila, H., Saari, M., Tuittila, E-S., Turunen,
1170 J., and Väliranta, M. M.: Spatially varying peatland initiation, Holocene development and estimated radiative forcing within a subarctic fen, Quaternary Sci. Rev., 248, 106596, https://doi.org/10.1016/j.quascirev.2020.106596, 2020.

Pirinen, P., Simola, H., Aalto, J., Kaukoranta, J.-P., Karlsson, P., and Ruuhela, R.: Climatological Statistics of Finland 1981–2010:, Reports 2012:1, Finnish Meteorological Institute, Helsinki, Finland, ISSN 0782-6079, 2012.

Räsänen, M., Aurela, M., Vakkari, V., Beukes, J. P., Tuovinen, J.-P., Van Zyl, P. G., Josipovic, M., Venter, A. D., Jaars, K.,
1175 Siebert, S. J., Laurila, T., Rinne, J., and Laakso, L.: Carbon balance of a grazed savanna grassland ecosystem in South Africa, Biogeosciences, 14, 1039–1054, https://doi.org/10.5194/bg-14- 1039-2017, 2017.

Räsänen, A. and Virtanen, T.: Data and resolution requirements in mapping vegetation in spatially heterogeneous landscapes, Remote Sens. Environ., 230, 111207, https://doi.org/10.1016/j.rse.2019.05.026, 2019.

Räsänen, A., Juutinen, S., Tuittila, E-S., Aurela, M. and Virtanen, T.: Comparing ultra-high spatial resolution remote-sensing methods in mapping peatland vegetation, Journal of Vegetation Science, vol. 30, no. 5, pp. 1016-1026. https://doi.org/10.1111/jvs.12769, 2019.

Rasilo, T., Prairie, Y. T. and del Giorgio, P. A.: Large-scale patterns in summer diffusive CH_4 fluxes across boreal lakes, and contribution to diffusive C emissions, Global Change Biol., 21, 1124-1139, doi:10.1111/gcb.12741, 2015.

R Core Team: R: A language and environment for statistical computing. R Foundation for Statistical Computing, Vienna, Austria, available at: https://www.R-project.org (last access: 1 October 2021), 2021.

Reichstein, M., Falge, E., Baldocchi, D., Papale, D.Iubinet, M., Berbigier, P., ... and Valentini, R. On the separation of net ecosystem exchange into assimilation and ecosystem respiration: review and improved algorithm. *Global change biology, 11*(9), 1424-1439. 2005.

~~Repola, J.: Biomass equations for Scots pine and Norway spruce in Finland. Silva Fennica, 43(4), 625-647, ISSN 0037-5330, 2009.~~ Richardson, A. D., Mahecha, M. D., Falge, E., Kattge, J., Moffat, A. M., Papale, D., ... and Hollinger, D. Y. Statistical properties of random CO_2 flux measurement uncertainty inferred from model residuals. *agricultural and forest meteorology, 148*(1), 38-50. 2008.

Rinne J., Tuovinen J.-P., Klemedtsson L., Aurela M., Holst J., Lohila A., Weslien P., Vestin P., Łakomiec P., Peichl M., Tuittila E.-S., Heiskanen L., Laurila T., Li X., Alekseychik P., Mammarella I., Ström L., Crill P., and Nilsson M. B.: Effect of the 2018 European drought on methane and carbon dioxide exchange of northern mire ecosystems. Phil. Trans. R. Soc., 375, B37520190517, https://doi.org/10.1098/rstb.2019.0517, 2020.

Sagerfors, J., Lindroth, A., Grelle, A., Klemedtsson, L., Weslien, P. and Nilsson, M.: Annual CO_2 exchange between a nutrient-poor, minerotrophic, boreal mire and the atmosphere, J. Geophys. Res., 113, G01001, doi:10.1029/2006JG000306, 2008.

Sepulveda-Jauregui, A., Walter Anthony, K. M., Martinez-Cruz, K., Greene, S., and Thalasso, F.: Methane and carbon dioxide emissions from 40 lakes along a north–south latitudinal transect in Alaska, Biogeosciences, 12, 3197–3223, https://doi.org/10.5194/bg-12-3197-2015, 2015.

Silfver, T., Heiskanen, L., Aurela, M., Myller, K., Karhu, K., Meyer, N., Tuovinen, J-P., Oksanen, E., Rousi, M. and Mikola, J.: Insect herbivory dampens subarctic birch forest C sink response to warming, Nat. Commun. 11, 2529, https://doi.org/10.1038/s41467-020-16404-4, 2020.

Strack, M. and Waddington, J. M.: Response of peatland carbon dioxide and methane fluxes to a water table drawdown experiment, Global Biogeochem. Cy., 21, GB1007, https://doi.org/10.1029/2006GB002715, 2007.

Tan, Z., Zhuang, Q. and Anthony, K. W.: Modeling methane emissions from arctic lakes: Model development and site-level study. Journal of Advances in Modeling Earth Systems, 7(2), 459–483. https://doi.org/10.1002/2014ms000344, 2015.

1210 Tan, Z., Zhuang, Q., Shurpali, N. J., Marushchak, M. E., Biasi, C., Eugster, W., and Anthony, K. W.: Modeling CO_2 emissions from Arctic lakes: Model development and site-level study. Journal of Advances in Modeling Earth Systems, 9(5), 2190–2213. https://doi. org/10.1002/2017ms001028, 2017.

Thornton, B. F., Wik, M. and Crill, P. M.: Climate-forced changes in available energy and methane bubbling from subarctic lakes, Geophys. Res. Lett., 42, 1936-1942, doi:10.1002/2015GL063189, 2015.

1215 Tranvik, L. J., Downing, J. A., Cotner, J. B., Loiselle, S. A., Striegl, R. G., Ballatore, T. J., Dillon, P., Knoll, L. B., Kutser, T., Larsen, S., Laurion, I., Leech, D. M., McAllister, S. L., McKnight, D. M., Melack, J., Overholt, E., Porter, J. A., Prairie, Y. T., Renwick, W. H., Roland, F., Sherman, B. S., Schindler, D. W., Sobek, S., Tremblay, A., Vanni, M. J., Verschoor, A. M., von Wachenfeldt, E. and Weyhenmeyer, G.: Lakes and Reservoirs as Regulators of Carbon Cycling and Climate, Limnol. Oceanogr., 54, 2298-2314, doi:10.4319/lo.2009.54.6_part_2.2298, 2009.

Venables, W. N. and Ripley, B. D.: Modern Applied Statistics with S, Fourth Edition, Springer, New York, 1220 https://doi.org/10.1007/978-0-387-21706-2, 2002.

Vicente-Serrano, S., Begueria, S. and Lopez-Moreno, J.: A Multiscalar Drought Index Sensitive to Global Warming: The Standardized Precipitation Evapotranspiration Index, J. Clim., 23, 1696-1718, doi:10.1175/2009JCLI2909.1, 2010.

Virkkala, A. M., Aalto, J., Rogers, B. M., Tagesson, T., Treat, C. C., Natali, S. M., Watts, J. D., Potter, S., Lehtonen, A., Mauritz, M., Schuur, E. A. G., Kochendorfer, J., Zona, D., Oechel, W., Kobayashi, H., Humphreys, E., Goeckede, M., Iwata, 1225 H., Lafleur, P. M., Euskirchen, E. S., Bokhorst, S., Marushchak, M., Martikainen, P. J., Elberling, B., Voigt, C., Biasi, C., Sonnentag, O., Parmentier, F. J. W., Ueyama, M., Celis, G., St.Louis, V.,L., Emmerton, C. A., Peichl, M., Chi, J., Järveoja, J., Nilsson, M. B., Oberbauer, S. F., Torn, M. S., Park, S. J., Dolman, H., Mammarella, I., Chae, N., Poyatos, R., López-Blanco, E., Christensen, T. R., Kwon, M. J., Sachs, T., Holl, D. and Luoto, M.: Statistical upscaling of ecosystem CO_2 fluxes across the terrestrial tundra and boreal domain: Regional patterns and uncertainties, Global Change Biol., 27, 4040-4059, 1230 doi:10.1111/gcb.15659, 2021.

Walter, K. M., Zimov, S. A., Chanton, J. P., Verbyla, D. and Chapin, F.S. III: Methane bubbling from Siberian thaw lakes as a positive feedback to climate warming, Nature, 443, 71-75, doi:10.1038/nature05040, 2006.

White, J. R., Shannon, R. D., Weltzin, J. F., Pastor, J., and Bridgham, S. D.: Effects of soil warming and drying on methane cycling in a northern peatland mesocosm study, J. Geophys. Res.- Biogeo., 113, G00A06, 1235 https://doi.org/10.1029/2007JG000609, 2008

Whiting, G. J.: CO_2 exchange in the Hudson Bay lowlands: Community characteristics and multispectral reflectance properties, J. Geophys. Res., 99, 1519–1528, https://doi.org/10.1029/93JD01833, 1994.

Wik, M., Crill, P. M., Varner, R. K. and Bastviken, D.: Multiyear measurements of ebullitive methane flux from three subarctic lakes, J.Geophys.Res.Biogeosci., 118, 1307-1321, doi:10.1002/jgrg.20103, 2013.

1240 Wik, M., Johnson, J. E., Crill, P. M., DeStasio, J. P., Erickson, L., Halloran, M. J., Fahnestock, M. F., Crawford, M. K., Phillips, S. C. and Varner, R. K.: Sediment Characteristics and Methane Ebullition in Three Subarctic Lakes, Journal of geophysical research. Biogeosciences, 123, 2399-2411, doi:10.1029/2017JG004298, 2018.

1245 Zhu, S., Clement, R., McCalmont, J., Davies, C. A., and Hill, T. Stable gap-filling for longer eddy covariance data gaps: A globally validated machine-learning approach for carbon dioxide, water, and energy fluxes. *Agricultural and Forest Meteorology, 314*, 108777, 2022.